UNIVERSITY OF CALIFORNIA
RIVERSIDE

Mechanisms of Microbial Survival

A Dissertation submitted in partial satisfaction
of the requirements for the degree of

Doctor of Philosophy

in

Biochemistry and Molecular Biology

by

Brandon Lathrop Gallaher

August 2014

Dissertation Committee
Dr. Neal L. Schiller, Chairperson
Dr. James Borneman
Dr. Katherine Borkovich

The Dissertation of Brandon Lathrop Gallaher is approved:

Committee Chairperson

University of California, Riverside

Acknowledgements

I would like to say thank you to my advisor, Dr. Neal Schiller. His continual guidance and support has been essential to this work and my success at the University of California at Riverside. I could not have asked for a more compassionate, diligent and encouraging mentor. Neal has been a friend, as well as an advisor and I will miss working together.

Thanks to Dr. Danh Do, my lab partner and friend. It has been a pleasure to work together and I have learned so much from our experience together. His constant drive to improve and seek new opportunities has influenced me to become a better student and scientist.

I want to thank my qualification committee members, Dr. Craig Byus, Dr. Manuela Martin-Green, Dr. Katherine Borkovich and Dr. James Borneman. I am grateful for the continual commitment by Dr. Borkovich and Dr. Borneman, both of which, served on my annual research assessment committee and on my defense committee. I am appreciative for their advice and assistance in improving this research.

Last, but not least, I would like to thank my whole family. Specifically, I'd like to thank my mom and dad, Treva and Gerry Gallaher, who have supported and encouraged me throughout my life. Also, I'd like to thank my brother, Huston Gallaher, who has provided addition encouragement. Thanks to my in-laws, Dan,

Marty, Kaitlin, Brock and Taylor Hartman, who have provided continual guidance and support. Finally, thanks to my wife, Brittany Gallaher, who has continually provided love and support throughout my graduate education.

Dedication

I would like to dedicate this dissertation to my wife, Brittany Gallaher, and my daughter Hartley Kait Gallaher. They have been a blessing on my life and I cannot imagine my life without either of you. Brittany has been a constant source of inspiration and encouragement throughout my undergraduate and graduate education. Her unwavering support and motivation has made this journey possible. Hartley joined us only 9 months ago, but she has provided extra incentive to complete my work during this homestretch. I love you both so much!

Table of Contents

List of Figures

List of Tables

Chapter 1 - An Introduction to Pseudomonas aeruginosa and Helicobacter pylori.

Background and literature review for Pseudomonas aeruginosa

Cystic fibrosis transmembrane conductance regulator (CFTR)

Cystic fibrosis transmembrane conductance regulator (CFTR) gene is located on the 7th human chromosome, is transcribed over a 250 kb region, and produces a 1480 amino acid protein. The protein consists of 12 transmembrane domains, 2 nucleotide-binding domains (NBD) and multiple phosphorylation sites. CFTR is an ATP Binding Cassette (ABC) transporter, which regulates chloride transport across the apical surface of epithelial membranes[1]. The activity of CFTR has been linked to the activity of other epithelial membrane transporters[2, 3]. It is believed that the CFTR channel is activated by ATP binding and hydrolysis, predominately at NBD1. CFTR is also activated by a combination of cAMP-dependent protein kinase (PKA) phosphorylation of serines in the R-domain, specifically 660, 737, 795, or 813, in addition to ATP binding at the NBDs and hydrolysis[4]. Inactivation of the CFTR channel is accomplished by dephosphorylation at the previously mentioned sites by protein phosphatase 2C (PP2C)[5].

Cystic fibrosis: Prevalence and significance

Cystic fibrosis (CF) is the most common autosomal recessive disease among Caucasians[6]. Mutations occur on the long arm of chromosome 7 within the CFTR gene. Mutated alleles occur in 1 in 25 individuals and the disease affects 1 in 2500 live births[6]. More than 1000 different mutations in the CFTR gene have been documented. Because of the broad influence of CFTR and its sheer size, mutations can have a variety

of effects on the protein's function and a broad spectrum of disease phenotypes[7-9]. Mutations in CFTR have been classified into 5 distinct groups which impact CFTR distinctly. Class I is characterized by mutations that result in the production of defective CFTR protein[8]. This defect is typically associated with InDels, nonsense or splice site mutations, which lead to truncated mRNA and the absence of CFTR protein[10]. These mutations account for approximately 5% of observed cases. Class II is characterized by successful protein synthesis but defective protein post-translational processing. This typically results in improper localization of the CFTR channel and possible degradation of the protein[10]. This class contains the most commonly observed mutation, seen in roughly 70% of cases, which is the deletion of phenylalanine at position 508[8, 11]. This deletion results in defective processing of the protein during biosynthesis and eventual proteolysis[6]. Class III mutations cause defective CFTR regulation, typically due to decreased affinity for ATP by the NBD. These result in the inability of CFTR channel to open and close appropriately and accounts for about 2% of cases[10]. The class IV mutations are characterized by defective conductance. Similar to class III mutations, the CFTR protein is properly synthesized and is successfully localized to the apical surface of epithelial cell membranes but the chloride current generated upon activation of the channel has a decreased flow. Mutations in class IV only account for ~1% of cases[8]. The final class, V, is dedicated to mutations which result in reduced amounts of CFTR proteins. This can be caused by decreased mRNA stability or mutations that destabilize the CFTR protein. These mutations are the least common and consist of less than 1% of CF cases[8]. Depending on the severity of the CFTR mutation, the phenotype observed

in the patient can vary, but includes some degree of abnormal secretions. The altered secretions impact the gastrointestinal tract by causing abnormal bile and pancreatic secretions, which lead to maldigestion, malabsorption and contribute to a variety of gastric complications[10]. The phenotypes of CFTR mutations are also experienced in the lungs of CF patients and as before, symptoms stem from abnormal secretions. In the lungs, altered secretions contribute to a viscous mucus secretion and an increased risk of chronic pulmonary infections.

Most CF patients suffer from a mutation at ΔF508 mutation. This mutation results in a significant decrease of CFTR at the apical surface of epithelial cells. In the lungs, this decrease results in high risk of chronic pulmonary infections due to reduced mucociliary clearance[11]. Early pulmonary infections are most commonly caused by *Staphylococcus aureus*, *Pseudomonas aeruginosa* and *Haemophilus influenzae*[11]. The most noteworthy is *P. aeruginosa*, since 80% of CF patients eventually become infected by this pathogen[11].

Pseudomonas aeruginosa: Epidemiology and cystic fibrosis pathology

P. aeruginosa is an opportunistic, gram negative, non-fermenting, aerobic, rod shaped, ubiquitous bacterium which measures 1-5 μm long by 0.5-1 μm wide. *P. aeruginosa* was originally identified by Carle Gessard in 1882 during his analysis of a greenish blue pustule. The bacterium was later associated with neonatal sepsis, burn sepsis, as well as acute and chronic lung infections. Over recent years, its association with human pathology has expanded. *P. aeruginosa* is the second most common cause of nosocomial pneumonia (17%), most of which are resistant to multiple antibiotic

treatments. *P. aeruginosa* is the third most common cause of urinary tract infections (7%), the fourth most common cause of surgical site infections (8%), the seventh most common bloodstream pathogen (2%), and the fifth most common bacteria isolated from infections overall (9%)[12]. While *P. aeruginosa* is associated with a wide array of human pathologies, it is probably best known for its infection of the lungs in CF patients. Infections by *P. aeruginosa* are the most common cause of respiratory failure in CF patients, as well as the leading cause of death. It is believed that individuals acquire the infection during early childhood, with a median age of 1 year[13]. Upon initial colonization by non-mucoid *P. aeruginosa,* inflammation is triggered by bacterial attachment to the epithelial surface and is spearheaded by neutrophil recruitment[14]. *P. aeruginosa* strains which do not produce alginate, an exopolysaccharide, are considered non-mucoid. *P. aeruginosa* infections which are capable of adapting to stresses within the CF lung typically form acute infections. Hypermutable *P. aeruginosa* strains are able to adapt to stresses and have a selective advantage in the CF lung. Increased reactive oxygen species, and induced SOS system contribute to an increased rate of mutation in the bacteria[15]. Hypermutable *P. aeruginosa* strains are more likely to develop multidrug resistance, aided by sublethal antimicrobial treatments, and are more likely to form persistent infections within the lungs[16-19]. During these persistent infections, genes associated with the acute infection are selected against[11], allowing the bacteria to convert to a chronic infection[20]. On average, after 11 years of recurrent acute infections or persistent infections by *P.* aeruginosa, CF patients develop a chronic infection of mucoid *P. aeruginosa.* The conversion is typically caused by a spontaneous

mutation in MucA, a regulator of alginate expression, resulting in the truncation of MucA that prevents its inhibition of the alginate biosynthetic pathway[21]. The mature alginate polymer is secreted out of the cell and forms a protective barrier that shields the bacteria from cellular stress, host immune response and harmful biochemicals including antibiotics. At this stage of infection the use of aggressive antimicrobial treatments has little success of eradicating these bacteria[6]. Attempts to utilize alginate lyase to improve the effect of antibiotics in vivo have encountered various complications including diminished enzyme activity, as well as stimulating a host immune response, though pegylation modifications of the enzyme have helped[22].

Pseudomonas aeruginosa: Alginate production and characteristics

Alginate is a slime-like exopolysaccharide composed of mannuronic and guluronic acids. The polymer is synthesized by the twelve gene alginate biosynthetic operon and, a single, separate, constitutively expressed gene, *algC*[23]. Expression of the alginate biosynthetic operon is regulated by a single sigma factor, σ^{22}, encoded by *algU*. During normal conditions, the MucA and MucB complex sequesters σ^{22} to the inner membrane. As mentioned previously, the conversion to alginate production is most commonly caused by a mutation of MucA, specifically at allele 22, which causes a premature stop codon, truncating MucA. The resulting protein is no longer able to bind σ^{22}, allowing it to induce expression of the alginate biosynthetic operon as well as transcriptional enhancer genes, *algB* and *algR*. A single promoter, pAlgD, is thought to control the entire operon, though there is recent evidence to suggest the role of internal promoters[24-26]. The biosynthesis of alginate begins in the cytoplasm with the

conversion of fructose-6-phosphate to GDP-β-D-mannuronic acid monomers via a series of modifications by AlgA, AlgC, and AlgD (Figure 1) [23, 27, 28]. These monomers are then polymerized into a long mannuronic acid (M) polymer and passed into the periplasm by Alg8, aided by Alg44[29]. It is hypothesized that the polymer is transported through a multi-protein periplasmic complex (MPC)(Figure 2) [30]. In the periplasm, the polymer becomes partially epimerized by AlgG[31, 32] to form guluronic acids (G), and partially acetylated on mannuronic acids by AlgF, AlgJ, and AlgI[33, 34]. It is thought that AlgK and AlgX are part of the periplasmic complex[35]. Recent studies, regarding AlgL (Alginate Lyase), have presented conflicting observations, which has raised further questions regarding its presence within the periplasm and its expression along with the biosynthetic pathway[36-40].

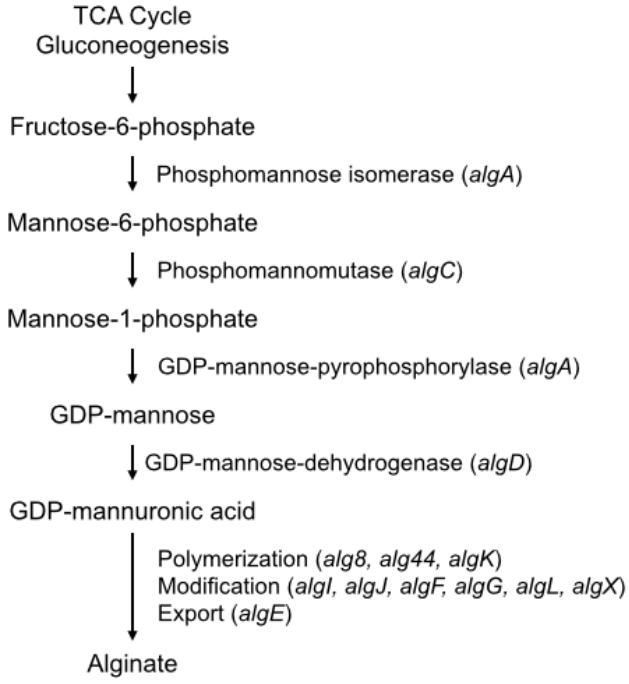

Figure 1. Alginate biosynthetic pathway. Starting from fructose-6-phosphate generate through gluconeogenesis to complete mature alginate.

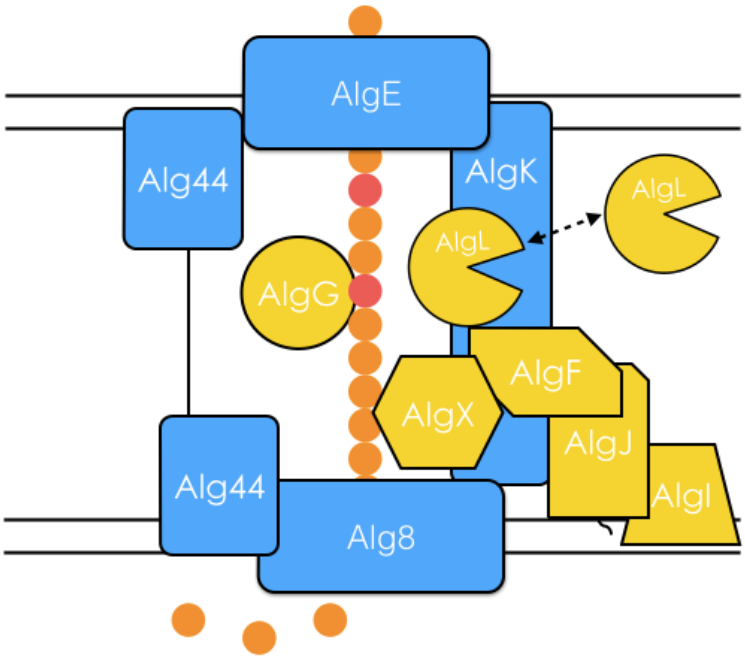

Figure 2. Putative multi-protein alginate biosynthetic complex. Composed of 9-10 different proteins consisting of alg8-algJ. The location of AlgL within this complex is one of the subjects of this dissertation.

Pseudomonas aeruginosa: Alginate Lyase

Alginate lyases are found in a diverse group of microorganisms as well as marine organisms such as algae and mollusks. Alginate lyases are present in both organisms which synthesize alginate and those which do not synthesize alginate. Organisms that do not produce their own alginate utilize the enzyme to breakdown exogenous alginate into a usable carbon source[41]. In organisms that synthesize alginate, the lyase is speculated to control the polymer length and might have a role in biosynthesis[42]. Alginate lyase enzymes can exhibit a variety of different specificities, including cleaving between (endo-type) either mannuronic blocks (M-M), guluronic blocks (G-G) or between mannuronic-guluronic blocks (M-G)[43]. Degradation by an endo-type lyase results in the

production of oligosaccharides of various sizes. Other enzymes exhibit an exo-type activity resulting in the production of degraded alginate monomers.

Alginate lyase (AlgL) in *P. aeruginosa* is an endomannuronic lyase, cleaving between blocks of mannuronic acids. AlgL is expressed in the alginate biosynthetic operon along with a bulk of the genes required for alginate synthesis. The AlgL mechanism proceeds by a β-elimination of the glycosidic 1-4 O-linkage between acids. Degraded polymers are eventually broken down into dimers and trimers and are not utilized by *P. aeruginosa* as a carbon source. Two crystal structures have been isolated, including a structure with a bound trisaccharide[44, 45]. The exact electron pushing mechanism for this reaction has not been determined. However, the structures have allowed us to identify various domains and residues that could participate in the β-elimination chemistry. The conserved domain, NNHSYW (190-195), and Y246, are thought to be involved in the β-elimination. N191 and H192 are thought to stabilize the sugars within the binding site, while Y246 initially deprotonates the C-5 position and then eventually donates the hydrogen to the glycosidic bond completing the cleavage. The resulting product is an oligomer with a 4-deoxy-L-erythro-hex-4-enepyranosyluronate at the nonreduced end[46].

It is accepted that the primary function of AlgL is to break down alginate polymers, but its co-expression with other components of the biosynthetic operon suggests that there might be an alternate function. Various studies have demonstrated the necessity for AlgL to be present and active for alginate production, speculating that AlgL could have a role in alginate production. AlgL could possibly be involved in

polymerization[36, 38, 47], or the regulation of polymer length during polymerization[48]. Other studies have observed alginate production in the absence of AlgL, suggesting that its primary role is to degrade trapped periplasmic polymers[37]. Although each study has provided some new insight, there seems to be very little consensus regarding its function within the biosynthetic operon, a question which requires further research to completely understand AlgL.

Pseudomonas aeruginosa: AlgX

AlgX is expressed in the alginate biosynthetic operon in *P. aeruginosa*. The protein is ~59 kDa before the removal of a periplasmic localization signal peptide leaving the protein at ~56 kDa[39]. The protein is essential for the synthesis of full sized alginate polymers, besides this, little else is known about the protein and its function[36, 39]. A recent study by Riley et al. determined the crystal structure of *P. aeruginosa* AlgX, which provided some insight to a possible role in acetylation of the alginate polymer[49]. Identification of the structure identified a two-domain protein with an N-terminal SGNH hydrolase-like domain and a C-terminal putative carbohydrate-binding module (CBM). Site directed mutagenesis of D174, H176, and S269 residues in the N-terminal domain) abolished acetylation of the polymer. Comparison to other SGNH hydrolase proteins confirmed the spatial arrangement of key residues within the SGNH hydrolase-like domain. The only significant difference between the AlgX SGNH hydrolase-like domain and other model SGNH hydrolase domains is the substitution of Asp328Tyr[49]. The putative C-terminal CBM is speculated to consist of two binding groups, two upstream lysine residues at 396 and 410, and a binding pocket consisting of 4 residues R364,

T398, W400, and R406. There have been no additional studies done to validate the role of the C-terminal CBM.

Driving Hypotheses for *Pseudomonas aeruginosa* AlgL

1. AlgL is a necessary component of alginate synthesis. An AlgL deletion would result in cells that are non-mucoid and do not produce detectable alginate.
2. AlgL's lyase activity is required for cell viability. Complementation of an *algL* knockout by a catalytically inactive AlgL would be insufficient to recover cell viability.
3. AlgL is an essential component of a periplasmic complex that aids the transport of alginate through the periplasm.

Driving Hypotheses for *Pseudomonas aeruginosa* AlgX

1. AlgX has the ability to bind the alginate polymers.
2. Site-directed mutagenesis of the AlgX C-terminal carbohydrate-binding module impacts alginate binding.
3. The ability of AlgX to bind alginate is essential to its function and alginate biosynthesis.

Background and literature review for Helicobacter pylori

***Helicobacter pylori*: History and Bacteriology**

Helicobacter pylori (*H. pylori*) is a microaerophilic, gram negative, helix-shaped bacteria. When growing conditions are not ideal, *H. pylori* forms coccoid cells that are more resistant to stress. The helical bacterium measures 3.5 microns long by 0.5 microns wide. It is believed that different strains of *H. pylori* have lived in human stomachs for over 58,000 years and genetic variations between strains have allowed for investigation of early human civilization migration patterns[50-52]. In 1982, Warren and Marshall cultured *Campylobacter pyloridis*, later reclassified as *Helicobacter pylori*, in vitro over 3-4 days on rich blood agar[53, 54]. Contrary to the accepted science at the time, they believed that *H. pylori* was a pathogenic gastric bacterium capable of causing gastric ulcers. However, due to the high frequency of asymptomatic infections, their findings were met with skepticism for three additional years, until Marshall and Warren demonstrated that *H. pylori* caused ulcers by validating Koch's postulates regarding infectious disease using a self-ingested experiment[55].

***Helicobacter pylori:* Prevalence and Pathology**

Today, *H. pylori* is the most common bacterial infection in humans[56, 57]; conservative estimates suggest that 50% of the world's population is infected by *H. pylori*[57]. The mode of transmission is not completely understood, though the consensus seems to be either fecal/oral or oral/oral dissemination[58]. There appears to be a link between transmission and socioeconomic standing[57, 59-61]. In developing nations, more than 50% of children are infected before the age of 10, and 80% of adults

are infected[57, 61]. In developed nations, infections in children are rare and the rate of infection increases with age peaking at 50% for individuals over 60 years of age[57]. While it initially seems that these statistics suggest a continuing rate of infection, recent epidemiology studies suggest that infection rates in adults are lower than that in children. It is postulated that the rates of infection in children are higher due to lower standards of hygiene[62]. In addition to hygiene, several other factors have been linked to higher rates of transmission, including overcrowding, bed sharing, siblings and house density[63-65].

A large majority of individuals infected by *H. pylori* will have no symptoms and will not develop symptoms. However, *H. pylori* has the potential to cause a variety of symptoms including bloating, loss of appetite, nausea, vomiting and peptic ulcers[55, 66]. *H. pylori* Infections are the leading cause of peptic ulcer disease (PUD) and are responsible for 80% of stomach ulcers and 90% of duodenal ulcers. Chronic type B gastritis can also lead to more severe medical conditions such as gastric adenocarcinomas, and B-cell mucosa-associated lymphoid tissue (MALT) lymphomas.

Three factors contribute to a majority of *H. pylori*'s virulence: urease activity, motility, and cellular adhesion. Disruption to any of these three factors prevents *H. pylori* colonization of the gastric milieu. Urease converts urea into CO_2 and ammonia. *H. pylori* also expresses a unique pH dependent urea channel, UreI, which allows for the permeability of urea at low pH and blocks urea permeability at favorable pHs. These two proteins, urease and UreI, work in harmony to produce a constant production of a cloud of ammonia, which neutralizes the acidic epithelium environment surrounding the

bacteria[66-68]. *H. pylori* has 2-6 unipolar sheathed flagella assisted by secreted mucolytic enzymes which facilitate movement through the thick gastric mucus[58]. Finally, *H. pylori* utilizes a variety of surface proteins including proteins from the Hop family, to attach to the epithelial cells. The most well-known adhesion protein is BabA, an outer membrane protein that binds to the fucosylated Lewis b (Le^b) histo-blood group antigen[66, 69-71]. Once bound to the cellular surface, a majority of *H. pylori* strains express *vacA*, an exotoxin, which inserts itself into the host epithelial cell membrane, forming a hexameric anion channel[72]. The channel is speculated to allow the influx of HCO_3^+, organic anions and bacterial nutrients[66]. In addition, VacA is also suspected to translocate to the mitochondria and cause the release of cytochrome c and the triggering of executioner caspase 3, eventually leading to epithelial cell apoptosis[66, 73]. Apoptosis can also be triggered through MHC class II molecules present on the epithelial cell surface[74]. Bacterial attachment to the cell surface stimulates the immune response, triggering the recruitment of neutrophils, T cells, B cells, and macrophages, resulting in chronic inflammation and additional epithelial cell damage[75].

Helicobacter pylori: Diagnosis and Treatment

The diagnostic techniques used to identify *H. pylori* infections are separated into invasive or non-invasive techniques. Non-invasive techniques include culturing or microscopic identification of bacteria from stool samples, urease breath tests, and detection of disease markers by antibody. Invasive techniques involve gastric biopsy by fiber optic endoscopy. The choice of test depends on numerous factors, which should be considered by the clinician in accordance with current American College of

Gastroenterology (ACG) guidelines[76]. Briefly, diagnosis of *H. pylori* infections for patients not already requiring endoscopy and having no previous record of infection is done by either urease breath test, stool antigens, or serology. Patients with a record of previous infections are diagnosed by detection of bacterial antigens in stool samples. Endoscopic biopsy is reserved for patients who have or have had a gastric ulcer or patients suspected of MALT lymphoma[76].

Once diagnosed, treatment begins with either a triple or a quadruple therapy depending on the prevalence of clarithromycin resistance, the latter being used when resistance is high. Triple therapy consists of a proton pump inhibitor, amoxicillin (β-lactam) and clarithromycin (macrolides) and is administered for 7-14 days[76]. Quadruple therapy includes bismuth, commercially known as Pepto-Bismol, a proton pump inhibitor, metronidazole (nitroimidazole), and tetracycline (polyketide) and is given for 10-14 days[77].

***Helicobacter pylori*: Emergence of antibiotic resistance**

The general development of antibiotic resistant bacteria is due to various factors including, non-compliance, improper prescription, and use of antibiotics in animal feed[78]. The resistance to antibiotics has been previously observed in *H. pylori* and has already been shown to impact treatment[79]. The development of antibiotic resistance in *H. pylori* is due to various factors including spontaneous mutations and the accumulation of DNA encoding resistance genes from other bacteria. *H. pylori* is well suited for genetic adaptation because the bacteria are naturally competent, able to assimilate naked DNA from its environment, and prone to frequent point mutations due to a lack of DNA repair

mechanisms, such as the mutS mismatch repair machinery[80-82]. This lack of DNA repair ultimately results in spontaneous mutations. Non-synonymous single nucleotide polymorphisms (SNPs) can occur in a wide variety of biological systems, which impact antibiotic resistance, including porin proteins, efflux complexes, and antibiotic targets, such as penicillin binding proteins.

Metronidazole mechanism of action and resistance

Recent research has identified mutations that impact *H. pylori* resistance to metronidazole. Metronidazole, first introduced in 1960, is a low molecular weight molecule that passively diffuses through the bacterial cell membrane, but is linked to intracellular reduction[83]. Once in the cell, the molecule localizes near pyruvate:ferrodoxin oxidoreductase and functions as an electron sink, capturing electrons from ferrodoxin, which normally reduces H^+ into hydrogen gas[83]. Pyruvate:ferrodoxin oxidoreductase is typically utilized by the bacterial cell to produce ATP. Because metronidazole passively diffuses through the membrane, intracellular reduction of metronidazole creates a driving gradient for additional metronidazole uptake. In the presence of oxygen, metronidazole functions as an electron donor and results in the formation of superoxide and non-reduced drug[84]. Activated metronidazole intermediates interact with host DNA causing nicks, DNA breaks, and destabilization of DNA helices throughout the genome[85, 86]. Resistance to metronidazole is attributed to mutations and inactivation in a pair of nitroreductases, *rdxA* and *frxA*, that contribute to the formation of active metronidazole. Mutations resulting in the inactivation of *rdxA* (type I) seem essential for metronidazole resistance,

whereas mutations in *frxA* alone are insufficient to cause resistance[87]. However, the combination of mutations in *rdxA* and *frxA* (type II) produce higher levels of resistance[87].

Clarithromycin mechanism of action and resistance

Clarithromycin binds to the 23S bacterial ribosomal RNA subunit of the 50S microbial ribosome and inhibits protein synthesis[88]. Commonly, resistance is gained by mutations, which reduces the binding of the antibiotic to the rRNA subunit[89]. The adenine to guanine mutation at 2143 is most frequent, observed in about 75% of resistant strains. A mutation of the neighboring adenine, 2142, to guanine mutation is observed only 21% of the time[79]. Clarithromycin resistance has been shown to decrease the eradication of infections by the initial triple therapy regimens but not subsequent treatments[79].

Tetracycline mechanism of action and resistance

Tetracycline is a broad-spectrum bacteriostatic antibiotic. Tetracycline is considered an ideal therapeutic because it is effective against most common pathogens, and has good oral absorption, with low toxicity and low cost[90]. Though the influx of tetracycline into the cell is still not completely understood, it is believed that the antibiotic entry into the cell is probably facilitated in a pH dependent manner. Once in the cell, tetracycline binds reversibly to various components of the bacterial ribosome. The most significant is tetracycline binding to the 30S ribosomal subunit which blocks aminoacyl-tRNA binding to the acceptor site in the ribosome. This binding inhibits the synthesis of bacterial proteins, preventing further growth[90]. Two primary mechanisms contribute to

tetracycline resistance: protection of the ribosome and decreased intracellular tetracycline concentrations. It is unclear how TetM and TetO provide tetracycline resistance, but the proteins share a number of properties with bacterial elongation factors including ribosome-associated GTPase activity[90] . Decreased influx and increased efflux can also significantly impact tetracycline sensitivity[91]. A combination of multi drug efflux systems including the Acr family of proteins and the MexAB-OprM complex[92], as well as tetracycline specific efflux mechanisms, TetR and TetA, contribute to resistance by decreasing cellular levels of tetracycline.

β-lactam mechanism of action and resistance

β-lactams are the most frequently prescribed antibiotics in the world[93] and represent numerous drugs containing the biochemical beta-lactam ring structure. Some examples of common β-lactams include penicillin, cephalosporin, ampicillin, and amoxicillin. β-lactams are transported into the periplasmic space of gram-negative bacteria through outer membrane porin proteins. β-lactams target the penicillin binding domains (PBD) of penicillin binding proteins (PBPs). PBPs are a family of proteins that are involved in bacterial cell wall biochemistry, including catalyzing the glycosidic linkage between NAM and NAG, the crosslinking between peptidoglycan chains, maintaining bacterial shape and facilitating cellular division[94]. PBPs contain two domains, a N-terminal transglycosylase domain and a C-terminal transpeptidase domain. Most bacteria express between 4 and 8 different PBPs[94]. β-lactams covalently bind to the C-terminal transpeptidase domain of PBPs, inhibiting the transpeptidase activity and

preventing formation of the fishnet-like cell wall structure. The lack of this structural crosslinking leads to loss of osmotic stability, and can lead to cell death[94].

Bacteria typically employ three different mechanisms to combat β-lactams: the breakdown of β-lactams, using β-lactamase; mutations in the C-terminal domain of PBPs; and mutations in outer membrane proteins which reduce permeability. The most common is expression of β-lactamase enzyme, which cleaves the β-lactam ring within the antibiotic, deactivating the molecule[93]. Bacteria either express β-lactamase from their genomic DNA or from a plasmid, the latter being the most common in gram-negative bacteria.

The outer membrane of bacteria forms a significant barrier to β-lactam permeation; the hydrophilic nature of some β-lactams allows diffusion through porins essential to entry into the periplasm[93]. The mutation of outer membrane porin proteins which exclude β-lactam drugs is another common mechanism of resistance.

Alterations of PBPs can lead to reduced affinity for β-lactams and increased resistance. However, PBPs have a limited distance of divergence as the function of penicillin binding proteins is essential to cell survival and mutations that would alter the function of PBPs would not be well tolerated.

The aim of this study is to address β-lactam resistance mechanisms in *H. pylori.* Of the aforementioned mechanisms of β-lactam resistance, *H. pylori* oddly lacks the most common mechanism, expression of a β-lactamase enzyme. On the other hand, *H. pylori* contains 4 PBPs[95], as well as a variety of outer membrane porin proteins[96]

and efflux proteins[97-99]. Previous studies have addressed specific mutations in PBPs and have characterized their impact on amoxicillin resistance[95, 96, 100-103]. However, the mutations in the PBP family do not account for the level of resistance observed in clinically isolated strains, suggesting that other mutations and mechanisms are contributing to higher levels of resistance.

Driving Hypotheses for *Helicobacter pylori*

1. Nucleotide mutations distinguish an in vitro generated amoxicillin resistant strain, IS5, from it's amoxicillin sensitive parental *H. pylori* strain, 26695.
2. The presence of non-synonymous single nucleotide polymorphisms (nsSNPs) in several IS5 proteins, specifically in outer membrane proteins, PBPs and efflux proteins, contribute to amoxicillin resistance.
3. Transformation of mutated genes into the sensitive 26695 background, significantly increase the resistance to amoxicillin.

Chapter 2 - The evolution of amoxicillin resistance in *Helicobacter pylori*

Abstract

Helicobacter pylori (*H. pylori*) is a gram negative, helix-shaped bacteria measuring 3.5 microns long by 0.5 microns wide. In 1982, Warren and Marshall demonstrated that *H. pylori* caused gastric ulcers by using a self-ingestion experiment. *H. pylori* is prone to frequent point mutations due to a lack of DNA repair mechanisms. The goal of this study is to quantitate the impact of non-synonymous single nucleotide polymorphisms on amoxicillin resistance. We examined the progression of spontaneous genetic mutations that contribute to amoxicillin resistance in H. pylori when exposed to increasing concentrations of amoxicillin in vitro. During the selection process, we isolated five strains each of which had progressively higher levels of resistance. Using a whole genome sequencing approach, we identified mutations in a number of genes, notably pbp1, pbp2, hefC, hopC, and hofH, and by sequencing these genes in each isolate we were able to map the order and gradual accumulation of mutations in these isolates. These five isolates, each expressing multiple mutated genes and four transformed strains expressing individually mutated pbp1, hefC, or hofH, were characterized using minimum inhibitory concentrations, amoxicillin uptake, and efflux studies. Our results indicate that mutations in pbp1, hefC, hopC, hofH, and possibly pbp2 contribute to H. pylori high-level amoxicillin resistance. The data also provide evidence for the complexity of the evolution of amoxicillin resistance in H. pylori and indicate that certain families of genes might be more susceptible to amoxicillin resistance mutations than others.

Introduction

Helicobacter pylori (*H. pylori*) is the most common bacterial infection in humans[56, 57]; conservative estimates suggest that 50% of the world's population is infected by *H. pylori*[57]. While a majority of the infections are asymptomatic, symptoms can consist of gastric ulcers, chronic type B gastritis which is linked to gastric adenocarcinomas and B-cell mucosa-associated lymphoid tissue (MALT) lymphoma[78]. *H. pylori* is the leading cause of peptic ulcer disease (PUD); peptic ulcers affect ~4.0 million people in the United States with roughly 350,000 new cases every year[104].

Previous studies have suggested the absence of the mutS mismatch repair mechanism in *H. pylori* leads to a higher rate of mutation[80]. A second study demonstrated that *H. pylori* infections treated with amoxicillin that were not completely eliminated, lead to persistent infection with an increased resistance to amoxicillin[105]. A portion of amoxicillin resistance has been associated, by previous study, to spontaneous mutations occurring within penicillin binding proteins (PBP1-3) and outer membrane proteins (Hop B and C) but these mutations do not completely account for the high level of resistance seen in some clinical strains[96, 100, 101, 103].

This study attempts to identify the various mutations that contribute to amoxicillin resistance in *H. pylori*. This was accomplished by passing a sensitive 26695 strain on progressively higher concentrations of amoxicillin. By repeatedly selecting for amoxicillin resistance, this study was able to isolate various in vitro evolved resistant strains. The identification of spontaneous mutations was achieved by whole genome sequencing comparing the genomes of a highly amoxicillin resistant isolate, IS5, to the amoxicillin

sensitive parental strain, 26695. This allowed for the identification of several mutations including some novel single nucleotide polymorphisms (SNPs), insertions and deletions (Indels). Further, traditional sequencing of intermediate isolates revealed the order that mutations occur. To validate the contribution of specific genes to amoxicillin resistance, mutated genes of penicillin binding protein 1 (*pbp1*), outer membrane protein 3 (*hofH*), a novel OMP, and putative RND efflux pump *hefC*[97], a novel efflux pump, were individually transformed into the sensitive parental strain 26695. Transformants were analyzed by minimum inhibitory concentration (MIC) to determine their contribution to amoxicillin resistance. Additional MIC analysis in the presence of efflux pump inhibitors (EFI), 1-(1-Naphthylmethyl)-piperazine (NMP) and Phenyl-arginine-β-napthylamide (PAβN), was used as a secondary method to validate the mechanism of contribution in isolated strains and individual transformants. These two EFIs have previously been reported to impact resistance-nodulation-cell division (RND) efflux systems in *E. coli*, reducing the MIC and cellular accumulation of various antimicrobial drugs and dyes, respectively[106].

Methods and materials

Creation of in vitro selected amoxicillin resistant strains from a sensitive strain: Creation of a series of resistant *H. pylori* 26695 strains was done by inoculating 26695 into a 96 well plate in serial two-fold dilutions of amoxicillin ranging from 16 mg/L to 0.006 mg/L. Wells were filled with 150 µL Brucella broth (Becton, Dickinson and Co.) containing 10% Fetal Bovine Serum (FBS) (Sigma Aldrich) and 1% IsovitaleX (Becton, Dickinson and Co). Wells were inoculated with log-phase bacteria (0.5-0.6 OD_{600}) at

1:100 fold dilution and were grown for 48-72 hours at 37°C in a humidified 10% CO_2 incubator. Each well of the 96-well plate was visually inspected for signs of growth. The culturing was repeated by inoculating another plate using the cells from the well with the highest amoxicillin concentration with observed growth. The replating was repeated over a nine-month period, resulting in an isolate with a maximum amoxicillin MIC of 4.0 mg/L.

Identification of genomic mutations distinguishing resistant and sensitive strains: IS5 and 26695 were cultured overnight on Brucella agar (Becton, Dickinson and Co.) supplemented with 5% sheep blood (Colorado Serum Co.) (Brucella blood agar) and 0.25 mg/L amoxicillin, if necessary. Cells were resuspended in sterile 0.01 M pH 7.4 phosphate buffer supplemented with 137 mM NaCl and 27 mM KCl, (PBS) and genomic DNA was isolated using the DNeasy Blood and Tissue kit (Qiagen), following manufacturer's specifications. A 5 µg aliquot of the resulting genomic DNA was sheared by sonication in order to create 400 bp DNA fragments. T4 DNA polymerase (New England Biolabs) and *E. coli* DNA polymerase I Klenow (New England Biolabs) were used to repair DNA overhangs and convert them into blunt-ends. A genomic library was created using an Illumina genomic sample prep kit, according to the instructions provided. Flow cell DNA adapters were ligated to the blunt-ends of the DNA fragments and purified using a PCR purification kit (Promega) allowing them to be hybridized to a flow cell. DNA fragments were submitted to the Integrative Institute of Genomic Biology (IIGB) and University of California at Riverside (UCR) for Illumina sequencing and genomic analysis. Genomic analyses resulted in short reads of approximately 32 bp and were assembled against a previously published NC_000915 *H. pylori* genomic

sequence[107]. This alignment resulted in 30x coverage over the entire genome. Following assembly, the department of Bioinformatics at UCR analyzed alignment for single nucleotide polymorphisms (SNPs) and insertions or deletions (InDels).

Benzylpenicillin [benzyl-^{14}C] potassium accumulation: Benzylpenicillin [benzyl-14C] potassium was used to measure the accumulation of amoxicillin within the *H. pylori* cell. Penicillin has previously demonstrated a similar binding affinity with PBP1 compared to amoxicillin[95, 100]. The strains 26695, IS3 and IS5 were grown to log-phase on Brucella blood agar and then suspended in PBS to a concentration of 3-5 x 10^9 cells/mL. The cells were then incubated with benzylpenicillin [benzyl-^{14}C] potassium (American Radiolabeled Chemicals) at 1 µCi/mL and 37°C in a humidified 10% CO_2 incubator for up to 30 minutes. Aliquots of 0.5 mL were removed at 1, 5, 10, and 30 minutes. The cells were washed twice with PBS to remove unbound antibiotic and subsequently resuspended in scintillation fluid at 1:100. Accumulation of benzylpenicillin [benzyl-^{14}C] potassium was determined by measuring counts per minute (CPM) using a Beckman LS6500 scintillation counter.

MICs of isolated strains in the presence of efflux pump inhibitor: To determine the contribution of efflux to amoxicillin resistance, the MIC of 26695, IS2, IS3, IS4, IS5 were determined in the presence of 1-(1-Naphthylmethyl)-piperazine (NMP) (Sigma Aldrich) or Phenyl-arginine-β-napthylamide (PAβN) (Sigma Aldrich). The MICs were performed according to the previously established microdilutional protocol[100]. Briefly, each strain was grown for 24-36 hours to an early log-phase on Brucella blood agar. Cells were suspended in Brucella broth supplemented with 10% FBS and 1%

IsovitaleX, to an optical density 600nm (OD_{600}) 0.4-0.5. Cells were used to inoculate 3 rows of a 96-well plate by adding 5 µL (~10^6 cells) aliquots to each well. Wells were also filled with 150 µL Brucella broth supplemented with 10% FBS and 1% IsovitaleX, in addition to amoxicillin concentrations between 1-8 mg/L in 0.5 mg/L increments, and with 100 mg/L NMP or 100 mg/L PAβN. Plates were incubated in a 37°C humidified 10% CO_2 incubator for 48-72 hours or until growth could be detected by measuring a significant change in OD_{600}.

PCR amplification of resistance genes and transformation into the parental 26695 strain: IS5 was cultured for 48 hours on Brucella blood agar supplemented with 0.25 mg/L amoxicillin and grown at 37°C in a humidified 10% CO_2 incubator. IS5 cells were isolated after 48 hours and suspended in sterile PBS prior to genomic DNA extraction using a DNeasy Blood and Tissue kit (Qiagen). PCR amplification of *pbp1* was accomplished by combining forward and reverse primers, to a final concentration of 0.2 µM, TGA TTG TCA TGG GGT TAT TAG CC (*pbp1*+) and GGG GGT TGA ATA GTA GGG GAT TTT (*pbp1*-), respectively, with ~100 ng genomic DNA, 3% Dimethyl sulfoxide (DMSO), 2x Apex Mastermix (Genesee Scientific). All primers were synthesized by Integrated DNA Technology (IDT). The PCR reaction resulted in a 1.9 kb fragment, which was verified by gel electrophoresis on a 1% w/v 89 mM Tris-Borate buffer supplemented with 2mM EDTA (TBE) agarose gel containing 0.5 mg/L ethidium bromide (EtBr). The PCR product was purified using the DNA Clean and concentrator kit (Zyppy). Purified DNA was sequenced at the Institute for Integrative Genome Biology (IIGB) at the University of California at Riverside by combining 0.83 µM forward primer, corresponding

to the amplified gene, with ~100 ng purified PCR product. Similar PCR approaches were used for *hofH*, *hefC*, and *pbp2*, producing PCR products with similar size using the following primers, ATA GGA GGC ATG GTG GGA TCT ATT (*hofH*+), GTC AGAG ATA AAG GGC GGG GAA (*hofH*-), CGT GGC GCT TTT CCC TAA AA (*hefC*+), CAC ACC AAA AAC CTC CCC C (*hefC*-), CCA CCT TAG AAG TAG TGC TGC C (*pbp2*+), and CTA ACA GGC CCC CTA GTT TTG AC (*pbp2*-), respectively. The resulting PCR fragments were then transformed into log-phase 26695 cells grown for 32 hours on Brucella blood agar at 37°C in a humidified CO_2 incubator. The preparation of electrocompetent cells and subsequent transformation of the PCR fragments was adapted from a previously published method by Wang et al[108]. Briefly, early-log phase 26695 cells were suspended in 20% glycerol and washed three times before separating into 100 µL aliquots. Each aliquot was combined with 500 ng purified DNA and electroporated in 2 mm gap electroporation cuvettes by a BTX ECM 630 electro cell manipulator at 2.5 Vk, 600 Ω, and 25 µF. Electrocompetent cells were resuspended in 400 µL SOC media and immediately plated on Brucella blood agar and recovered for 24-48 hours or until growth was observed in a 37°C humidified CO_2 incubator. Cells were scraped from the plate and suspended in 500 µL sterile PBS then plated on Brucella blood agar supplemented with either 0.125 mg/L or 0.250 mg/L amoxicillin. The plates were incubated for 48-72 hours or until colonies were observed in a 37°C humidified CO_2 incubator; individual colonies were isolated and replated on identical agar to maintain the mutants.

Screening and MIC characterization of 26695 mutant isolates: The mutated genes corresponding to each transformed strain were PCR amplified using the above protocol and subsequently purified using the DNA Clean and concentrator kit (Zyppy). Purified PCR products were then sequenced, as before, at the IIGB at UCR using the forward primer. The resulting sequences were compared to the parental strain, 26695, gene sequence. Once confirmed, transformants were subjected to microdilutional MIC assays, as described above[95]. Each strain was grown as before to an early log-phase on Brucella blood agar. Cells were suspended in Brucella broth supplemented with 10% FBS and 1% IsovitaleX, to an optical density 600nm (OD_{600}) 0.4-0.5 and used to inoculate rows of a 96-well plate by adding 5 µL (~ 3 x 10^6 cells) aliquots of suspended cells to each well. Wells were also filled with 150 µL Brucella broth supplemented with 10% FBS and 1% IsovitaleX, in addition to amoxicillin in a serial two-fold dilution ranging from 0.003-16.0 mg/L. Plates were grown at 37°C in a humidified 10% CO_2 incubator for 48-72 hours or until growth was observed. The MIC was determined by measuring growth by OD_{600}.

MIC of mutation transformants in the presence of EFI: As before, transformants were grown in Brucella blood agar supplemented with 0.125 mg/L amoxicillin for 24-36 hours at 37°C in a humidified 10% CO_2 incubator, suspended in Brucella broth with 10% FBS and 1% IsovitaleX to an OD_{600} between 0.4-0.5. Wells of a 96-well plate were filled with Brucella broth, amoxicillin and inoculated as before, however, this time each sample was also supplemented with 100 mg/L NMP. The plates

were incubated at 37°C in a humidified 10% CO_2 incubator for 48-72 hours. Growth was determined by significant changes in OD_{600} as previously mentioned.

Results

In vitro evolution and whole genome sequencing: The in vitro evolution of sensitive *H. pylori* 26695 was accomplished by repeatedly passing a culture in progressively higher concentrations of amoxicillin over a nine-month period. During that time, 5 isolates, IS1-IS5, were isolated. The strains ranged in MIC from 0.5 mg/L to 4.0 mg/L, respectively, (Figure 3). IS5, the most resistant strain and the parental strain, 26695, were subsequently sequenced using Illumina whole genome sequencing. This analysis resulted in identification of roughly 80 mutations, both SNPs and InDels. Mutations that occurred in non-coding regions, didn't result in amino acid changes or were located in the last 6 amino acids of the coding region were eliminated. The remaining 24 mutations were sequenced in the sensitive and resistant strain to confirm the mutation, of which, 13 were false positives, leaving 11 mutations (Table 1). Previous studies have investigated the impact of mutations in penicillin binding protein 1 (PBP1), penicillin binding protein 2 (PBP2) and outer membrane protein 20 (Omp20 or HopC) on amoxicillin sensitivity[96, 100, 101]. This study identified two mutations in PBP1, at P372S and T438M, occurring in IS1 and IS4 respectively. One mutation was observed in PBP2 (E536K) and HopC (R302H), occurring at IS5 and IS2 respectively. This study was also able to identify a mutation upstream of 3-methyl adenine DNA glycosylase and a frame shift mutation in colicin V. Two additional point mutations were observed in the IS2 strain, G434W, in Nhac; Na+/H+ antiporter, an anion permease, and D98Y, in the

post-translation regulator of Flagellin A (FlaA). Two novel mutations in a multi-drug efflux protein (AcrB or HefC), D131E and L378F, occur in IS2 and IS3, respectively. Another novel mutation occurs in outer membrane protein 3 (Omp3 or HofH), G228W, occurring in IS5. In all, these mutations have inspired the further investigations of this study.

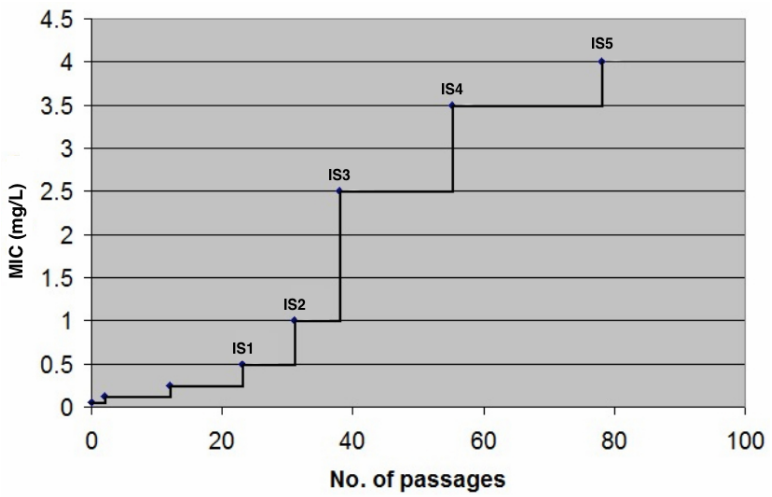

Figure 3. Evolution of amoxicillin resistance in H. pylori 26695 by sequential passage in increasing levels of amoxicillin. At various levels of amoxicillin resistance, bacteria were isolated and colony purified, starting with isolate IS1 with a MIC of 0.50 mg/L and ending with IS5 with a MIC of 4.0 mg/L.

Table 1. Mutations in nine genes, which potentially confer amoxicillin resistance to *H. pylori*. MIC determinations and presence of various mutations, which appeared in isolates IS1 to IS5. The bold + sign indicates the mutation first occurred in that isolate.

Gene	Mutation	Locus	Gene description	26695	IS1	IS2	IS3	IS4	IS5
MIC mg/L				0.06	.5	1	2.5	3.5	4
HP0597	T438M	631507	Penicillin Binding protein 1	-	-	-	-	**+**	**+**
HP0597	P372S	631706	Penicillin Binding protein 1	-	**+**	**+**	**+**	**+**	**+**
HP0602	70 bp upstream	638854	3 methyl adenine DNA glycosylase	-	-	-	**+**	**+**	**+**
HP0607	D131E	643852	Acriflavine resistance protein HefC	-	-	**+**	**+**	**+**	**+**
HP0607	L378F	644591	Acriflavine resistance protein HefC	-	-	-	**+**	**+**	**+**
HP0912	R302H	966081	Omp 20 (Hop C)	-	-	**+**	**+**	**+**	**+**
HP0946	G434W	1007964	Putative Nhac; Na+/H+ antiporter	-	-	**+**	**+**	**+**	**+**
HP0958	D98Y	1017441	Posttranscriptional regulator of Fla A	-	-	**+**	**+**	**+**	**+**
HP1565	E536K	1647429	Penicillin Binding Protein 2	-	-	-	-	-	**+**
HP0181	Indel	188235	Putative colicin V protein	-	**+**	**+**	**+**	**+**	**+**
HP1167	G228W	1233499	Putative Omp 3 (Hof H)	-	-	-	-	-	**+**

Benzylpenicillin [benzyl-^{14}C] potassium accumulation in IS3 and IS5: There was a significant ($p < 0.1$) decrease in accumulation between 26695 and IS5, at each time point examined. There was also a noted decrease between IS3 and 26695 at each time point though not statistically significant ($p > 0.1$), (Figure 4). These results suggest the involvement of either an outer membrane porin protein, such as HopC or HofH, which prevents the permeation of penicillin or efflux pump proteins, such as HefC, that aids resistance by reducing cellular levels of antibiotics.

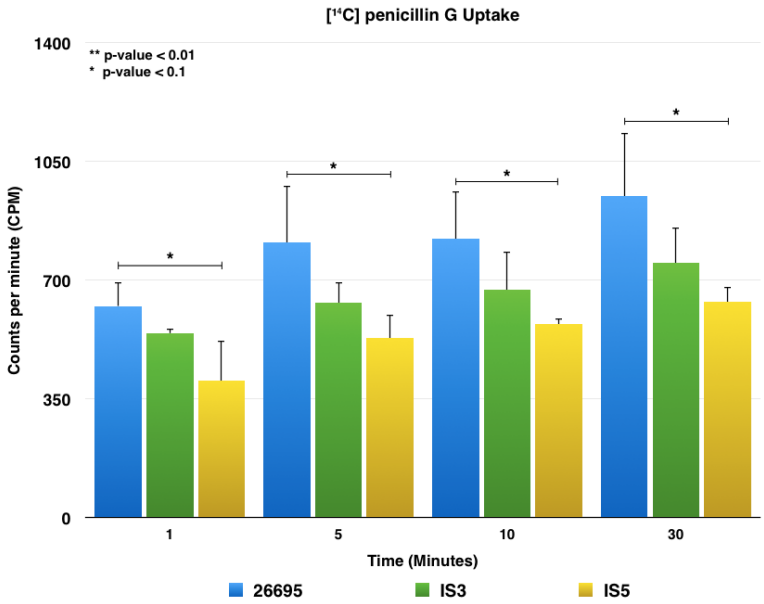

Figure 4. Isolates IS3 and IS5 accumulate less [14C] penicillin G than 26695 at each time point examined. Data shown represent the mean ± standard deviation based on at least 3 separate experiments. Statistical numbers represent p-values determined using the student t-test between respective samples.

The MICs of 26695 isolates with EFI: MIC analysis of IS2, which contains mutations in PBP1 (P372S), HopC (R302H), and HefC (D131E), was not affected by the presence of NMP. Isolate strains IS3, IS4 and IS5 each carry additional mutations in HefC (L378F), PBP1 (T438M), as well as, mutations in PBP2 and HofH. IS3, IS4, and IS5 strains grown in the presence of either efflux pump inhibitor (EFI), NMP or PAβN, exhibited a reduced level of amoxicillin resistance; IS3 MIC was reduced from 2.5 mg/L to 1.5 mg/L, IS4 from 3.5 mg/L to 2.5 mg/L and IS5 from 4.0 mg/L to 3.0 mg/L (Table 2). The parent strain 26695 was unaffected by the presence of either EFI.

Strain	MIC without EFI	MIC with PAβN	MIC with NMP
26695	0.06	0.06	0.06
IS2	1.0	ND	1.0
IS3	2.5	1.5	1.5
IS4	3.5	2.5	2.5
IS5	4.0	3.0	3.0

Table 2. MIC values (mg/L) of various isolates for amoxicillin in the presence or absence of an efflux pump inhibitor (EFI) at 100 mg/L. Each MIC was determined by calculating the p-values between the average OD_{600} of samples compared to the 26695 control; p-values < 0.05 represented growth. ND, not done. Representative of at least 3 replicates of this experiment.

Isolation of transformed 26695 strains and characterization by MIC: To better appreciate the contribution of single mutations on amoxicillin resistance, studies were initiated to transform mutations in *pbp1*, *hofH*, *hefC* and *pbp2* into the sensitive 26695 background. Transformants were created by allelic exchange with a PCR fragment carrying the proper mutation. After several attempts, only transformants in *pbp1*, *hofH*, and *hefC* could be isolated and verified by sequencing. Transformants were characterized by measuring the amoxicillin MIC in the presence of amoxicillin using the previously mentioned microdilutional protocol[100]. Transformants carrying the PBP1 mutations (PBP1-T), P372S and T438M, lead to an 8-fold increase in amoxicillin resistance (0.06 to 0.5 mg/L) whereas HofH transformants (HofH-T) with the G228W mutation and HefC transformants (HefC-T) with the L378F and D131E mutations, lead to a 16-fold increase in amoxicillin resistance (0.06 to 1.0 mg/L) (Table 3). HefC transformants carrying only the mutation at L378F was almost as effective as the double mutation in conferring amoxicillin resistance, suggesting at most a minor role for D131E mutation in amoxicillin resistance.

Strain	Mutations	MIC without NMP	MIC with NMP
26695	Parental	0.06	0.06
PBP1-T	T438M P372S	0.5	0.5
HofH-T	G228W	1.0	0.25
HefC-T	D131E L378F	1.0	0.06
HefC-LF-T	L378F	0.5	0.06

Table 3. MIC values (mg/L) of 26695 and transformants of 26695 for amoxicillin in the presence or absence of NMP, an efflux pump inhibitor, at 100 mg/L. Representative of at least 3 replicates of this experiment. Each MIC was determined by calculating the p-values between the average OD_{600} of samples compared to the 26695 control; p-values < 0.05 represented growth.

Impact of EFI on the MIC of transformants: The MIC of transformants PBP1-T, HofH-T, and HefC-T was determined in the presence of NMP at 100 mg/L. PBP1-T, with both P372S and T438M mutations, was not affected by NMP (Table 3). The HofH-T strain, grown in the same concentration of NMP, had a 4-fold reduction in MIC (1.0 to 0.25 mg/L) in the presence of NMP (Table 3). The HefC-T strain, with both D131E and L378F mutations, in the presence of NMP, demonstrated a dramatic 16-fold decrease (1.0 to 0.06 mg/L) while the HefC-LF-T strain containing the single L378F mutation had an 8-fold decrease in MIC (Table 3).

Discussion

In vitro generated resistant isolates: This study aimed to identify mutations that contribute to amoxicillin resistance in *H. pylori* 26695. This was achieved by growing a sensitive 26695 strain in the presence of amoxicillin over nine months. The results identified five distinct stages of resistance. The five isolated stages contained a total of eleven mutations in nine different genes. The first isolated strain, IS1, contained two of

the eleven mutations. One mutation is in PBP1 at P372S and the other mutation is a deletion of a cytosine in Colicin V protein, causing a frame shift. The mutation in Colicin V causes the normal stop codon to be shifted out of frame and synthesis extends from an 86 amino acid peptide to a 226 amino acid peptide. This likely prevents the protein from functioning properly. However, Colicin V is an unlikely candidate to contribute to the MIC of 0.5 mg/L amoxicillin.

Conversely, the mutation in PBP1 is located adjacent to the putative SAIK penicillin-binding motif (PBM)[101]. The P372S mutation potentially prevents Serine 368 from binding to amoxicillin. In addition, PBP1 is a likely candidate to have mutations that impact β-lactam resistance as previous studies have made reference to other mutations in PBP1 that have influenced resistance[96, 101, 103, 109-115].

IS2 contains four additional mutations, a significant increase from IS1, and achieves a MIC of 1.0 mg/L. In the IS2 strain the first of two mutations in HefC was observed. HefC is believed to function together with HefA and HefB to form an efflux pump complex[116]. Based on preliminary homology modeling of HefC, the sequence shares 26% sequence identify to MexB (according to PDB sequence blast), a protein that forms a homotrimer as a component of the MexAB-OprM multi-drug efflux pump in *P. aeruginosa*[117]. However, the D131E mutation in HefC does not significantly change the amino acid side chain and is not predicted to drastically impact side chain chemistry and function. The second mutation in IS2 occurs in HopC and is a R302H mutation. HopC is an outer membrane protein previously associated with amoxicillin resistance. Previous work demonstrated that a premature stop codon at amino acid 211 in HopC

reduces penicillin accumulation and increases the MIC[96]. The last two mutations observed in IS2, D98Y and G434W, occur in a posttranslational regulator of Flagella A protein (FlaA) and Na+/H+ antiporter (Nhac), respectively. While neither protein has ever been associated with β-lactam resistance, a prior study demonstrated the differential expression of various *H. pylori* genes when exposed to amoxicillin. Notable were two genes involved in flagella synthesis, *flgG* and *pflA*, as well as at least five other transport proteins[118]. In addition, proton flow is a critical component to a number of efflux pump systems in gram negative bacteria[119].

The largest jump in MIC was observed between IS2 and IS3, where the MIC jumped from 1.0 mg/L to 2.5 mg/L. The IS3 strain contains only two new mutations, one in the region upstream of 3-methyl DNA glycosylase and the second mutation in HefC. The mutation observed near 3-methyl DNA glycosylase could occur in the promoter and impact gene expression. The role of 3-methyl DNA glycosylase functions as a DNA repair enzyme and lower expression levels might diminish DNA repair, increase the mutation rate in *H. pylori* and aid cell adaptation. However, 3-methyl DNA glycosylase itself has not been directly linked to amoxicillin resistance.

The L378F mutation in HefC is the second mutation observed in this protein and the most likely to contribute to the increase in MIC seen in IS3. As mentioned before, HefC is predicted to form a homotrimer and is a component in an efflux pump complex with HefA and HefB[116]. The L378F mutation introduces a large hydrophobic side chain located on a helix toward the inner cavity of the homotrimer that could impact a nearby

putative β-lactam binding pocket[120]. Mutations in HefC are intriguing because this is a non-synonymous SNP that improves the efflux pump, increasing the efflux of amoxicillin.

IS4 contains only a single new mutation, occurring in PBP1 at T438M. This mutation has been previously identified and characterized by our lab and its contribution to amoxicillin resistance has been reported[96, 101]. Briefly, the mutation from threonine to methionine introduces a much larger side chain that is suspected to extend into the putative binding pocket and by doing so, restricts β-lactam binding. As expected, due to the mutation, there was a modest increase in MIC from 2.5 mg/L to 3.0 mg/L.

IS5 contains the final two mutations, one in PBP2, E536K, and one in HofH, G228W. IS5 displays a MIC increase from 3.0 mg/L to 4.0 mg/L amoxicillin. The mutation in PBP2 has been previously identified in an amoxicillin resistant strain[103]. However, the mutation was present with other mutations and it is unclear whether this mutation, alone, contributed to amoxicillin resistance. HofH, a putative outer membrane protein, is likely to impact amoxicillin sensitivity. This is significant since HofH has not previously been associated with amoxicillin resistance in *H. pylori*.

Penicillin accumulation and efflux pump inhibition of isolated strains: It was imperative to characterize the isolate strain mutations further. This was done by measuring the MICs of IS2-IS5 in the presence of efflux pump inhibitors NMP and PAβN. Strains IS2-IS5 contain mutations in an efflux pump, HefC. As previously mentioned, NMP and PAβN have been shown to influence the efflux of antibiotics and dye, however, the two inhibitors seem to have different mechanisms as their impacts on efflux vary[106]. In the presence of NMP, IS2, which contains the D131E mutation in HefC,

shows no change in MIC, remaining at 1.0 mg/L. On the other hand, strains IS3, IS4 andIS5, which contain both mutations in HefC, D131E and L378F, saw a significant MIC reduction in all three isolates, decreasing from 2.5 mg/L to 1.5 mg/L, 3.0 mg/L to 2.0 mg/L and 4.0 mg/L to 3.0 mg/L, respectively. This suggests that the D131E mutation alone in HefC does not significantly impact amoxicillin resistance. This also supported the hypothesis that the mutations in HefC impacted amoxicillin efflux, and more specifically that the L378F mutation is pivotal for resistance.

Analysis of PBP1, HefC and HofH transformants by MIC: Additional analysis of PBP1, HofH and HefC mutations was achieved by creating individual transformants in 26695. Using allelic exchange, linear fragments of DNA from IS5 were transformed into amoxicillin sensitive strain 26695. Transformants were selected on low levels of amoxicillin (0.125-0.250 mg/L). HefC mutations D131E and L378F were initially transformed together. A second transformant was created containing only L378F so that the contribution of this mutation could be determined independently from the D131E mutation. The MIC of each transformant was similar at 1.0 mg/L and 0.5 mg/L, for the double mutant, D131E and L378F, and single mutant, L378F, respectively. These values represent a 16-fold and 8-fold increase over parental levels, respectively. When these strains were grown in the presence of NMP, there was a drastic drop in MICs to 0.06 mg/L amoxicillin, identical to parental strain sensitivity levels. These results strongly suggest that the L378F mutation, in HefC, is sufficient to increase amoxicillin resistance in *H. pylori* 26695 and it does so by increasing the efflux of amoxicillin. The second mutation at D131E synergistically increases the MIC of the L378F transformant, but only

marginally. A similar analysis was done for PBP1. A single transformant was created and contained both of the observed PBP1 mutations. The transformant demonstrated an 8-fold increase in resistance, increasing from 0.06 to 0.5 mg/L. Attempts to create a HofH mutation were successful and the transformant demonstrated a 16-fold increase in amoxicillin MIC compared to the parental levels. Unfortunately, the attempts to create a PBP2 transformant in the sensitive 26695 strain were unsuccessful. This could mean that this mutation alone is not impactful enough to increase the MIC of the sensitive strain to a level of 0.125 or 0.250 mg/L, the amount used in the agar selection plates. Nevertheless, PBP2 could work synergistically with other mutations in the penicillin binding protein family to induce higher levels of resistance.

Conclusion: Ultimately, this study was able to create a series of amoxicillin resistant *H. pylori* 26695 isolates utilizing in vitro selection in Brucella media supplemented with amoxicillin. Using a combination of whole genome Illumina sequencing and traditional sequencing, this study was able to identify 11 mutations, in 9 genes, that distinguish the parental strain, *H. pylori* 26695, from the resistant strains, IS1-IS5. By referencing recent publications and using microdilutional minimum inhibitory concentration (MIC) assays, with and without efflux pump inhibitors (EFI), this study was able to identify specific mutations in IS1-IS5, which contribute to amoxicillin resistance (Figure 5). Among those mutations, mutations in PBP1, at P372S, HefC, at L378F, and HofH, at G228W, were not previously documented and are believed to contribute to amoxicillin resistance. Transforming individual mutations in PBP1, HefC and HofH into the sensitive parental strain further validated these contributions to amoxicillin

resistance. These transformants were characterized by MIC with and without EFIs. The results supported the discovery of novel mutations and their contribution to amoxicillin resistance. While other unidentified mutations could contribute to amoxicillin resistance, the identified mutations are considered to contribute the majority of the resistance observed in IS5, our most resistant, in vitro isolate.

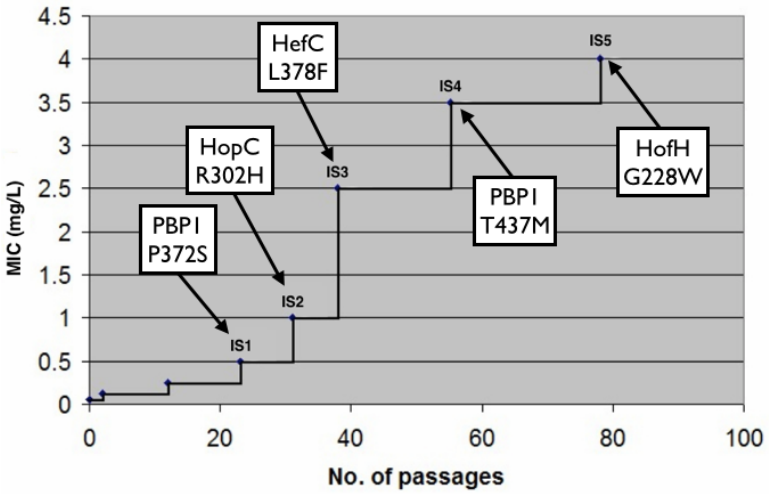

Figure 5. Evolution of amoxicillin resistance in H. pylori 26695 by sequential passage in increasing levels of amoxicillin. At each step of resistance, mutations that are thought to contribute to the increased amoxicillin resistance are indicated.

Chapter 3 - The role of alginate lyase for alginate biosynthesis in Pseudomonas aeruginosa

Abstract

Pseudomonas aeruginosa is a gram-negative aerobic bacillus that is ubiquitous in nature and found in soil and water. *P. aeruginosa* is an opportunistic bacterium associated with pulmonary infections in cystic fibrosis (CF) patients. In the lungs of CF patients, *P. aeruginosa* activates an alginate biosynthetic operon. Alginate is a polymer of mannuronic and guluronic acid that is exported from the cell and forms a mucous (slime) layer. The mucous causes respiratory complications and reduces the efficacy of antibiotic regimens.

Alginate Lyase, AlgL, is expressed in a twelve-gene alginate biosynthetic operon consisting of *algD*, *alg8*, *alg44*, *algK*, *algE*, *algG*, *algX*, *algL*, *algI*, *algJ*, *algF*, and *algA* genes. Previous studies have outlined a putative scaffolding complex, which is thought to contain AlgG, AlgK, AlgX, AlgE, Alg44, Alg8 and AlgL. This research addressed the paradoxical expression of AlgL, an endo-mannuronic alginate lyase protein, during alginate biosynthesis. In an attempt to investigate the role of AlgL, this study created algL knockout strains. Initially, two distinct phenotypes were observed, a viable, non-alginate producing phenotype, FRD5434, and a lethal, alginate producing phenotype, FRD5431. Upon further investigation, FRD5431 could be rescued by in-trans complementation of algL. Surprisingly, expression of catalytically inactivated algL mutants in FRD5431 was able to recover parental levels of alginate production but not viability. These findings suggest that AlgL might have a structural role in the alginate

biosynthetic complex. However, attempts to identify protein-protein interactions with the biosynthetic complex using MudPIT MS-MS were unsuccessful.

Introduction

Pseudomonas aeruginosa is a non-fermenting, gram-negative, opportunistic pathogen, which is found throughout the environment. Since the introduction of anti-staphylococcal drugs, *P. aeruginosa* has become the most important bacterial infection in individuals suffering from cystic fibrosis (CF). CF affects 1 in 3000 individuals and is caused by a variety of mutations in the cystic fibrosis transmembrane conductance regulator (CFTR)[121]. The most common mutation in CFTR is a deletion of F508, which results in the misfolding of the protein and proteolysis[10]. CFTR is a regulated chloride channel that is localized to the apical surface of epithelial cells[6]. While the disease impacts the secretions from the gastrointestinal tract, the pancreas, and even the male reproductive tract, the most significant impact is on the lungs[10]. The absence of CFTR results in improper fluid transportation and the build-up of thick mucus in the lungs[6]. This altered lung environment allows for the colonization of various bacteria, most importantly *P. aeruginosa*. Infections start in early childhood and over time, due to re-infection, develop into chronic infections that are difficult to eradicate[10]. Progression to a chronic infection is concurrent with *P. aeruginosa*'s constitutive production of alginate. Alginate is an exopolysaccharide, which forms a barrier around the bacteria, protecting from host immune responses and chemical therapeutics.

Production of alginate is achieved by expression of the twelve-gene alginate biosynthetic operon consisting of *algD, alg8, alg44, algK, algE, algG, algX, algL, algI,*

algJ, algF and *algA* and a single separately expressed gene, *algC* (Figure 6). Alginate lyase (AlgL) is an endomannuronic lyase expressed in the biosynthetic operon and preliminary studies have provided conflicting findings. Initial studies by Schiller and Monday[36, 47] observed the absence of alginate production in a transposon generated *algL* knockout strain. This pioneering work provided the first evidence suggesting that AlgL was required for alginate production. This work was later confirmed by a second *algL* knockout created by Albrecht et al[38]. This study demonstrated that catalytically inactive AlgL proteins were not able to recover alginate production in *algL* knockouts. At the same time, a third knockout was generated by Jain et al[37]. This study produced a knockout that was able to produce alginate but was unable to survive. Alginate production was speculated to accumulate in the periplasmic space, leading to membrane lysis and cell death.

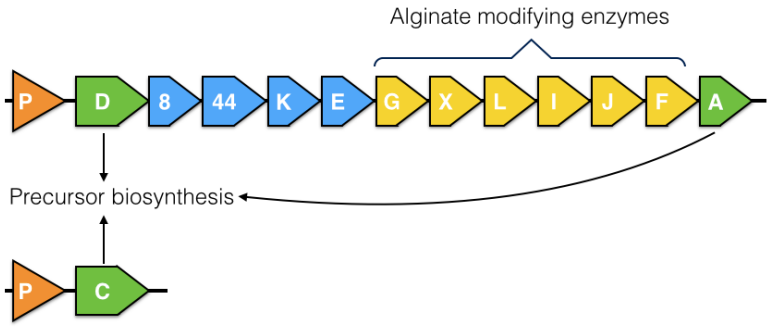

Figure 6. Alginate biosynthetic operon and separately expressed algC. Green, involved in precursor formation. Blue, involved in polymerization and export. Yellow, involved in modification of the polymer.

In an attempt to resolve the conflicting findings of these previous studies, this study aimed to create a unique *algL* knockout to determine the phenotype independently. These studies also aimed to expand on the previous research by attempting to detect

protein-protein interactions with AlgL. As with the previous studies, initial attempts to create a non-polar *algL* knockout in the mucoid FRD1 strain were unsuccessful because the genotype was believed to be lethal. To circumvent this obstacle, the clinically isolated strain was modified by replacing the alginate biosynthetic operon promoter, pAlgD with a pTac promoter, creating FRD1050[37]. The new, inducible background, was used to create the two previous knockouts by Jain and Albrecht[37, 38] as well as the knockouts in this study.

Methods and Materials

Triparental mating of pMA5, an allelic exchange vector, into FRD1050 to create the *algL*Δ: To create the *algL* knockout we used triparental mating[122]. This method requires three different bacteria, serving three functions: the donor, Gene Hog (Invitrogen) strain of *E. coli* carrying the allelic exchange vector, pMA5, which is the pEX100T plasmid[38, 123] containing an algX-Gm^R-algI DNA fragment, expressing the gentamicin resistance cassette in the place of *algL*; the helper, HB101 carrying pRK2013[122] to facilitate plasmid transfer; and the recipient, FRD1050[37]. The three strains are initially grown independently in Luria Broth (LB) (Becton, Dickinson and Co.) with 50 µg/mL tetracycline (LB Tc_{50}), 200 µg/mL kanamycin (LB Kn_{200}), and without selection (LB), respectively. Equal (200 µL) aliquots of the three strains were then combined in 2 mL LB before transferring cells onto a 0.45 µm filter paper, using a Swinnex® filter holder. The strains were grown together, on the filter, overnight at room temperature (25-27°C). This allowed for the exchange of genetic material through cell-to-cell junctions and the transfer of the plasmid containing the *algL* knockout to FRD1050.

The strains were resuspended in 5 mL of 0.85% w/v sterile saline and screened for gentamicin resistance on *Pseudomonas* Isolation Agar (PIA) (Becton, Dickinson and Co.) supplemented with 100 µg/mL gentamicin (PIA Gm_{100}). Individual colonies were isolated and screened by PCR. Individual colonies were isolated and passed on PIA Gm_{100}; residual bacteria, remaining on the applicator, were screened by resuspending them in 0.2 µM of each primer, *algL+*, 5'-ATG AAA ACG TCC CAC CTG ATC C, *Gent-*, 5'-CGA TCT CGG CTT GAA CGA A, and *algLInt-*, ACC GCC CAG TCG AAG AGG TC, 3% DMSO and 2x Apex Mastermix (Genesee Scientific). A confirmed merodiploid colony was grown overnight in LB supplemented with 100 µg/mL gentamicin (LB Gm_{100}). The culture was subsequently plated on PIA Gm_{100} supplemented with 10% sucrose. The presence of sucrose induces the second crossover. Verification of the knockouts was done by isolation of genomic DNA from potential knockout colonies using the DNeasy Blood and Tissue Kit (Qiagen), following manufacturer's specifications. The DNA was screened by PCR, using the three-primer PCR approach described previously. The colony screening PCRs were assessed by gel electrophoresis using 1% agarose in 89 mM pH 8.3 Tris-borate buffer supplemented with 2 mM EDTA (TBE). The gel was supplemented with 0.5 µg/mL ethidium bromide (EtBr) prior to solidification. In addition, the PCR products were sequenced at the Institute for Integrative Genome Biology (IIGB) at the University of California at Riverside (UCR), using Primer A, to confirm the exchange of *algL* with *algL*Δ and the orientation of the gentamicin cassette within the alginate operon.

Characterization of FRD1050Δ*algL*: Knockout candidates were initially plated on PIA Gm_{100} supplemented with 0.5 mM IPTG to determine the induced phenotype. Two phenotypic populations were identified within the 16 colonies plated, lethal and viable. Two colonies were chosen to represent the two populations; these candidate colonies and FRD1050 (parental strain) were induced in liquid culture to assess uronic acid production as well as to analyze AlgL expression and activity. A single colony of each strain was used to inoculate 3 mL LB Gm_{100} cultures, and grown overnight at 37°C at 250 rpm. The resulting cultures were diluted 1:20, grown to early log-phase (0.4-0.5 OD_{600}) and induced with 0.5 mM Isopropyl β-D-1-thiogalactopyranoside (IPTG). The OD_{600} was measured at 1, 3, 4, 5, and 6 hours post-induction to quantitate cell growth. At those times, 10 mL culture aliquots were removed to measure uronic production and lyase activity. Each aliquot was centrifuged at 9,000 x g and 4°C for 20 minutes. The supernatant was retained and the cell pellet was washed three times with cold 0.01M pH 7.4 phosphate buffered saline (PBS), 137 mM NaCl and 27 mM KCl, before being resuspended in 50 mM Tris buffer pH 7.4 supplemented with 150 mM NaCl and 0.1% Triton-X 100 at 1/100 culture volume and subjected to temperature shock protein extraction[124]. The extracted protein was screened for lyase activity using the previously published thiobarbituric acid (TBA) assay [125]. The retained supernatant was screened for uronic acid by the carbazole assay[126, 127].

Rescue of alginate production in *algL* knockouts by expression of *algL* in-trans: To confirm that *algL* was the only gene affected by the allelic exchange, the FRD1050Δ*algL* needs to be recoverable by replacement of only *algL*. For this rescue

experiment *algL* was re-introduced on a low copy, high expression vector, pNLS18, created by Monday and Schiller[36]. Initially, the vector was purified from DH10β *E. coli* cells using Wizard® Plus SV Miniprep kit (Promega) and following the manufacturer's recommendations. The purified plasmid was then transformed into electrocompetent GeneHog® cells (Invitrogen) prepared as previously described[128]. This was accomplished by combining 100 µL electrocompetent GeneHog® cells with ~50 ng purified plasmid. The mixture was transferred to a 2 mm gap electroporation cuvette and incubated for 10 minutes at 0°C before being shocked at 2.5 kV, 150 Ω, and 25 µF by a BTX ECM 630 electro cell manipulator. The cells were immediately resuspended in 500 µL cold SOC media (Sigma Aldrich) and incubated for an additional 5 minutes at 0°C before recovering at 37°C for 1 hour with agitation. Transformed cells were spread, at various volumes on Luria Agar (LA) supplemented with 50 µg/mL tetracycline (LA Tc_{50}). Individual colonies were screened using the three-primer PCR approach described above. Once confirmed, the vector was moved into the FRD1050Δ*algL* cells by triparental mating. For this mating experiment the donor is GeneHog® cells, carrying the pNLS18 complementation vector, the helper is HB101 carrying pRK2013 to facilitate plasmid transfer, and the recipient is FRD1050Δ*algL* cells. The triparental mating and transfer of the pNLS18 into the *algL* knockouts occurred as described above. Briefly, each strain was grown separately in LB, using appropriate selection. The cultures were then combined on a 0.45 µM filter (Millipore) and grown together overnight at room temperature. The cell mixture was then resuspended from the filter, and spread on PIA

Tc_{100} Gm_{50} for selection of transformants. Isolated colonies were screened by PCR, to ensure maintenance of pNLS18, using the previously established three-primer PCR. Confirmed transformants were induced, as before, and screened for uronic acid production and lyase activity.

Transformation of pMAH202Q and pMAY256F into the induced lethal FRD1050Δ*algL* knockout: Mobilization of plasmids expressing mutated AlgL into *P. aeruginosa* was accomplished by triparental mating, as before. GeneHog® cells maintaining pMAH202Q and pMAY256F served as the donors, FRD5431, the induced lethal FRD1050Δ*algL* served as the acceptor, and HB101 cells maintaining pRK2013 acted as the helper. The strains were grown and mated as previously described. Cells were resuspended from the filter and selected on PIA Tc_{100} Gm_{50}. After selection, candidate transformants were screened using the previously mentioned PCR protocol with *algL+*, 5'-ATG AAA ACG TCC CAC CTG ATC C, *Gent-*, 5'-CGA TCT CGG CTT GAA CGA A, and *MCS-*, 5'-GT GCG GGG CTC TTC GCT. Primers A and B are designed to detect the gentamicin cassette within the *algL* knockout and Primers A and C are designed to detect the *algL* gene present on the complementation vector. The resulting PCR products were assessed by gel electrophoresis on a 1% TBE gel supplemented with EtBr.

Characterization of induced lethal FRD1050Δ*algL* complemented by *algL* point mutants: Confirmed transformants were used to inoculate 2 mL LB Tc_{100} Gm_{50} cultures. The cultures were incubated overnight at 37°C with agitation. The overnight

cultures were split and used to inoculate separate 20 mL LB cultures supplemented with 100 µg/mL tetracycline and 50 µg/mL gentamicin. The cultures were grown at 37°C with agitation to early log phase, 0.3-0.5 OD_{600}; one culture was induced with 0.5 mM IPTG, the other remained uninduced. At 1, 3, 4, 5, 6 hours, 2 mL aliquots were removed from the main cultures. Cells were separated by centrifugation at 9,000 x g for 20 minutes at 4°C. The supernatant was retained so that the uronic acid concentration could be determined using the carbazole assay[126]. In addition, periplasmic proteins from the isolated cells were extracted using temperature shock extraction[124], as before with the *algL* knockout, and analyzed for any residual lyase activity by TBA assay, as previously performed.

Periplasmic protein samples were analyzed by western blot to ensure expression and localization of the mutated AlgL to the periplasm. Briefly, protein samples were combined with an equal volume of 2x Laemmlie buffer supplemented with 5% β-mercaptoethanol. Samples were denatured by boiling for 10 minutes and allowed to cool to room temperature. Samples were loaded into the wells of a 10% polyacrylamide gel with a 1.5 cm 5% stacking gel, prepared as described in Current Protocols in Protein Science[129]. Samples were run through the stack at ~60 V, after which, the samples were separated for approximately 1 hour at ~120 V. The proteins were subsequently transferred for ~2 hours to a 0.45 µm nitrocellulose membrane (Bio-Rad). The membrane was blocked for 1 hour with 50 mM pH 7.6 Tris buffered saline, 150 mM, (TBS) supplemented with 0.1% tween-20 and 5% Apex® dry non-fat milk (bTBS) (Genesee Scientific). Following blocking, the membrane was quickly washed twice with

TBS supplemented with 0.1% Tween-20 (tTBS) for 5 minutes then incubated overnight at room temperature with a similar solution containing 5% dry non-fat milk and rabbit polyclonal anti-AlgL IgG[130] at 1:2000 dilution. The following day, the membrane was thoroughly washed for three times with tTBS for 10 minutes each. The membrane was then incubated for 3 hours with bTBS with goat anti-rabbit AP-linked IgG (Cell Signaling) at 1:2000 dilution. Finally, the membrane was washed three times with tTBS for 10 minutes, as before, and developed with BCIP/NBT substrate solution (Perkin Elmer) until bands appeared, typically 5-10 minutes. The developing reagent was removed by washing the membrane 3 times with 10 mL deionized water for 1 minute.

Creating an affinity HA-tagged *algL* pRK415 construct: Creating a tagged *algL* construct was done by PCR cloning of *algL* from FRD1 into pRK415. The PCR reaction consisted of 100 ng FRD1 genomic DNA, 3% DMSO, and 2x Apex Taq Mastermix (Genesee Scientific) and 0.2 µM of each forward and reverse primer. The forward primer, *XbaI_algL+*,5'-CGC GCG TCT AGA GAA AAC GTC CCA CCT ATC C, anneals to the 5' of *algL* (underlined), and adds an *Xba*I restriction site. The reverse primer, *algL_HA_EcoRI*, 5'-CCG CCG GAA TTC TCA GGC CTA GTC CGG CAC GTC GTA CGG GTA GGA TCC ACT TCC CCC TTC GCG GCT anneals to the 3' end of *algL* just upstream of the stop codon (underlined). It contains an extended region coding a hemagglutinin-tag (HA) and an *Eco*RI restriction site for cloning. The resulting product was confirmed by gel electrophoresis on a 1% TBE gel supplemented with EtBr. Once confirmed, the product was purified using a Zymo DNA clean and concentrator™ kit,

following manufacturer's specifications. The DNA was subsequently digested in parallel with pRK415, a low copy, high expression shuttle vector. Digestion of the PCR fragment and plasmid was done by incubating ~1 µg DNA with 5 µL 10x BSA, 5 µL 10x buffer #2 (New England Biolabs), 2 µL *Xba*I and 2 µL *Eco*RI (New England Biolabs). The total reaction volume was adjusted to 50 µL using nuclease-free water. The reaction was incubated at 37°C overnight and then purified using the Zymo DNA clean and concentrator™ kit, following manufacturer's specifications. The two purified fragments were then ligated together using T4 ligase. Insert and vector were combined in an 8:1 ratio along with 1 µL 50mM ATP, 10x T4 Ligase Buffer, and T4 Ligase (New England Biolabs), following manufacturer's specifications. The reaction was incubated overnight at room temperature before electroporation. The newly formed plasmid was called pBLHA (HA-tagged). Approximately 75 ng ligation reaction was combined with 100 µL electrocompetent GeneHog® cells. The cells were prepared as previously mentioned, following the European Molecular Biology Laboratory (EMBL) protocol[128]. Electrocompetent cells and ligation mixture were incubated on ice for 10 minutes in a 2 mm gap electroporation cuvette before being pulsed at 2.5 kV, 150 Ω, and 25 µF. The transformation was selected on LA Tc_{50} supplemented with 1 mM IPTG and 20 µg/mL X-Gal. White colonies were isolated the next day and PCR screened using the forward and reverse primers above. Once confirmed, individual colonies were used to inoculate a culture used for triparental mating.

Expression and isolation of AlgL-HA in FRD5431: pBLHA was transformed into FRD5431 by triparental mating, as described above. Candidate colonies were screened for the plasmid using three-primer PCR approach discussed above. Primers, *algL+, Gent-*, and *algLInt-*, were used to detect the gentamicin cassette and the pBLHA plasmid. A confirmed individual colony was used to inoculate 5 mL LB supplemented Tc_{100} Gm_{50} culture. The culture was grown overnight at 37°C with agitation. A 2 mL aliquot was used to inoculate a 100 mL LB Tc_{100} Gm_{50}. Cells were grown to early log-phase, 0.3-0.5 OD_{600}, then induced with 0.5 mM IPTG for 18-24 hours. Cells were isolated by centrifugation at 7000 x g for 20 minutes at 4°C. Pelleted cells were washed three times with cold 0.01 M PBS, and finally resuspended in 5 mL PBS supplemented with 100 mM $MgCl_2$ and 0.1% triton-X 100. The resuspension was sonicated 4 times for 20 seconds each using pulses with 50% duty cycle. Cells were centrifuged at 10,000 x g for 20 minutes to separate insoluble debris and soluble protein. Prior to analysis by western blot, soluble protein samples were concentrated by centrifugation using an Amicon® Ultracel® Filter device (Millipore) with a 30 kDa MWCO. Protein samples were concentrated to a fifth of their original volume (5-fold).

Crosslinking and immunoprecipitation of AlgL-HA: Isolation of protein-protein interactions was achieved by combining 200 µL concentrated protein extract with 10 µL 100 mM Disuccinimidyl suberate (DSS) (Thermo Scientific Pierce) in DMSO to a final concentration of 5 mM. The crosslinker, featuring an 11.4 Å arm, was allowed to react with the crude protein extract for 30 minutes at room temperature. The crosslinking reaction was quenched by adding 35 µL 300 mM pH 7.6 Tris buffer supplemented with

0.9 M NaCl and the reaction was allowed to sit at room temperature for 30 minutes. Once quenched, 5 µL rabbit IgG HA-tag monoclonal antibody (Cell Signaling Technology®) was added to the mixture and incubated overnight with agitation at 4°C, as recommended by the manufacturer. The protein-antibody mixture was then combined with 20 µL Dynabeads® Protein G. The beads were previously prepared by washing them 3 times with 0.5 mL 25 mM pH 5.0 citric acid buffer supplemented with 50 mM dibasic sodium phosphate, as recommend by the manufacturer. Beads were separated using a 1.5 mL MagneSphere® Technology Magnetic two-position Separation Stand (Promega). After washing, the Dynabeads® were resuspended in a 100 µL aliquot of the protein-antibody mixture. The Dynabeads® were allowed to incubate and capture the IgG antibodies overnight at room temperature with agitation. Beads were separated on the magnetic stand for 2 minutes with gentle aspiration. The residual unbound protein was removed and retained. The beads were washed three times for 2 minutes with 200 µL 25 mM pH 5.0 citric acid buffer supplemented with 50 mM dibasic sodium phosphate and 0.1% tween-20. The proteins were eluted from the beads with 100 µL 0.1 M pH 3.0 citric acid buffer. The mixture was allowed to incubate for 10 minutes with agitation before isolation of the elution. The resulting samples were analyzed by western blot to verify protein enrichment and to identify potential crosslinked products.

2D-LC (MudPIT) Q-TOF mass spectroscopy (MS) analysis of enriched crosslinked AlgL-HA: Identification of co-immunoprecipitation products with AlgL, was done, in collaboration with Dr. Songqin at the IIGB, using MudPIT MS-MS. Analysis of

protein mixtures required the digestion of proteins into smaller analyzable polypeptides by protease. Digestion by trypsin was used to yield ideal polypeptide fragments, 10-20 amino acids in size[131]. Digested polypeptides were separated into 5 fractions on two C18 chromatography columns (2D LC) using a combination of high and low pH reverse phase chromatography[132]. The fractions were then ionized by electron spray ionization and analyzed by quadrupole-time of flight (Q-TOF) mass spectroscopy at the IIGB. MASCOT database was used to match the spectra of polypeptide fragments detected by MS with a library of known spectra and proteins.

Results

Creation of two distinct algL knockouts by allelic exchange: Transformation of pMA5 into FRD1050 was accomplished by triparental mating. The initial single, crossover of pMA5 and FRD1050 genomic DNA results in a merodiploid colony containing both wild-type (WT) and knockout mutant *algL* (KO) genes. Confirmation of this initial crossover was done by PCR. The three-primer scheme, detailed above in the Material and Methods, allowed for identification of the WT *algL* gene and the KO *algL* gene containing the gentamicin cassette. Screening of four mucoid colonies resulted in two distinguishable bands for each colony, 690 bp and 968 bp, corresponding to the WT *algL* and KO *algL*, respectively. A PCR confirmed mucoid merodiploid colony was isolated and used to create the knockout strain by inducing a second crossover. An overnight merodiploid culture was selected on media containing 10% sucrose, which is lethal to cells containing *sacB*, a gene present on the exchange vector, pMA5. Selection for transformants on both gentamicin and sucrose selects for the second crossover

event, which is essential for cells to survive. The only viable recombination results in excision of both the WT *algL* and the exchange vector. This leaves the KO mutant *algL* gene, containing the gentamicin cassette in place of the WT *algL*, and completes the knockout. The second crossover was verified by screening the colonies, as before, using the three-primer PCR scheme discussed above. As expected, the 690 bp band, which corresponds to the WT gene is absent from the PCR, confirming that the WT gene has been successfully removed. Sequencing of the 960 bp PCR fragment generated from potential knockout colonies confirmed the insertion of the gentamicin cassette within the *algL* gene.

FRD1050Δ*algL* phenotype characterization: PCR-confirmed *algL* KO colonies were replica plated with and without induction to determine their viability and mucoid phenotype. Only 4 of the 16 colonies isolated could grow on media supplemented with 0.5 mM IPTG. Two colonies were chosen to represent the two observed populations, FRD5431, a strain that was lethal when induced, and FRD5434, a strain that was viable when induced. Growth curve studies, in the presence or absence of IPTG, were used to compare the parental strain, FRD1050, to FRD5431 and FRD5434. Each strain grew over the first 3 hours. After 3 hours, a significant decrease in OD_{600} and viable cell count was observed for induced FRD5431, compared to induced FRD1050 and induced FRD5434, (Figure 7 and 8). The strains were screened for alginate production, using the uronic acid assay mentioned above. Induced FRD5434 culture produced no detectable alginate, suggesting that alginate production has been impacted by mutagenesis (Figure 9). Conversely, a small amount of alginate was detected in the induced FRD5431

culture. Both knockout cultures were also screened for lyase protein and lyase activity using the TBA assay; minimal lyase activity was detected in either culture (Figure 10).

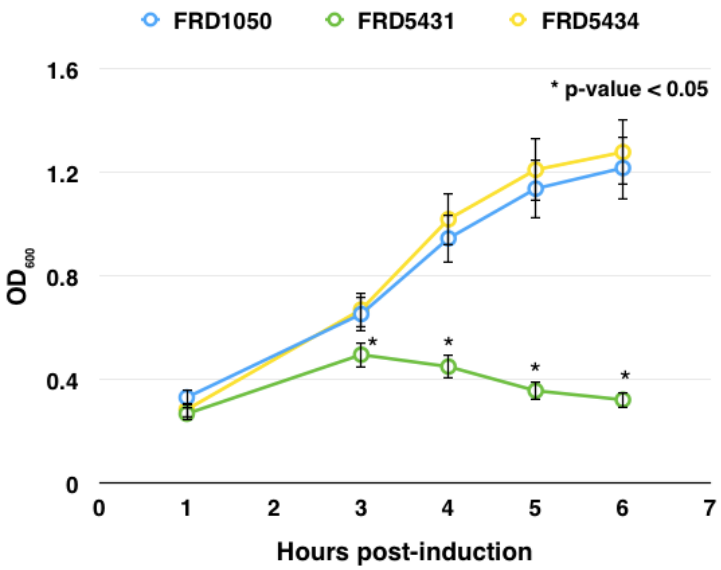

Figure 7. OD600 growth curve of the viable (FRD5434) and non-viable (FRD5431) FRD1050ΔalgL strains. The two KOs are compared to the parent strain, FRD1050. .

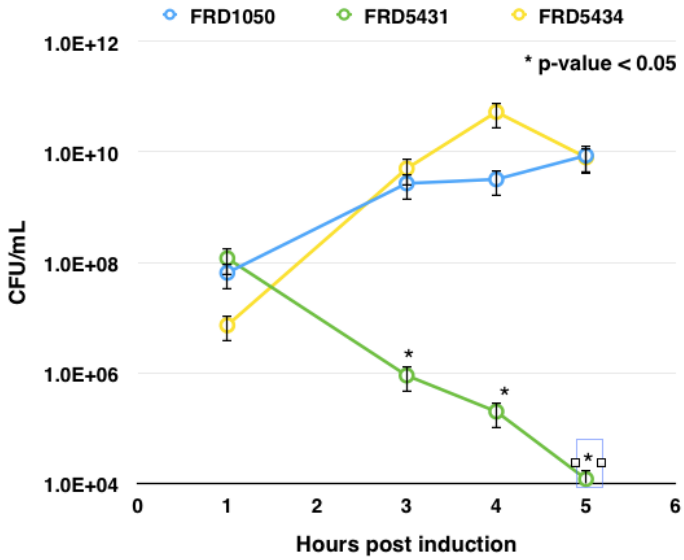

Figure 8. Viable cell counts of the viable (FRD5434) and non-viable (FRD5431) FRD1050ΔalgL strains. The two KOs are compared to the parent strain, FRD1050. Values represent the average of at least three replica experiments.

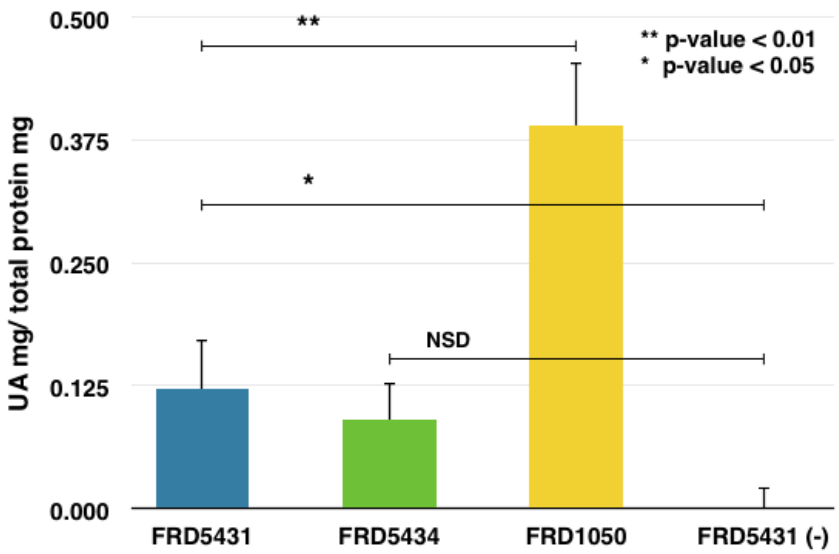

Figure 9. Uronic acid assays detecting total uronic acid production at various time points throughout the growth curve of FRD5431, FRD5434 and FRD1050, each induced with IPTG. FRD5431 (-) represents uninduced result. Values represent the average of at least three replica experiments.

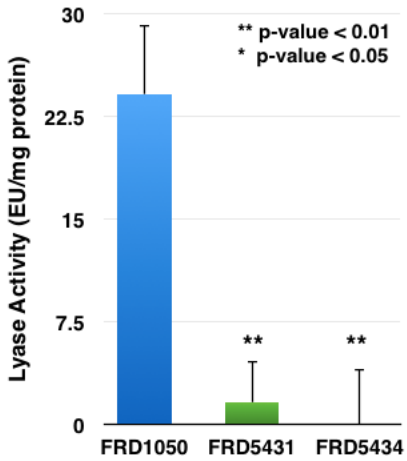

Figure 10. Lyase activity detected in FRD5431 compared to FRD1050. Values represent at least three replica experiments.

Complementation by pNLS18 and pMAH202Q and pMAY256F: To demonstrate that uronic acid production could be recovered by reintroducing *algL*, in-trans, a vector expressing only *algL*, pNLS18, was transformed into the knockouts, FRD5434 and FRD5431. Transformation of pNLS18 into both knockouts was

accomplished through triparental mating. Individual colonies were isolated and screened for the plasmid using the three-primer PCR approach, discussed above, which resulted in the re-emergence of the 690bp band, corresponding to the WT *algL* gene. Transformed colonies were induced with 0.5 mM IPTG; FRD5434:pNLS18 colonies remained non-mucoid when induced, compared to FRD5431:pNLS18 colonies, which recovered their viability and their visibly mucoid phenotype, (Figure 11 and 12). Analysis of complemented FRD5431:pNLS18 supernatant, by uronic acid assay, confirms that the cells were able to recover 85% of uronic acid production with respect to the parent, FRD1050 (Figure 13). Analysis of protein extract from FRD5431:pNLS18 demonstrated a significant increase in lyase activity, out producing the parent strain, FRD1050, by 2-fold, (Figure 14).

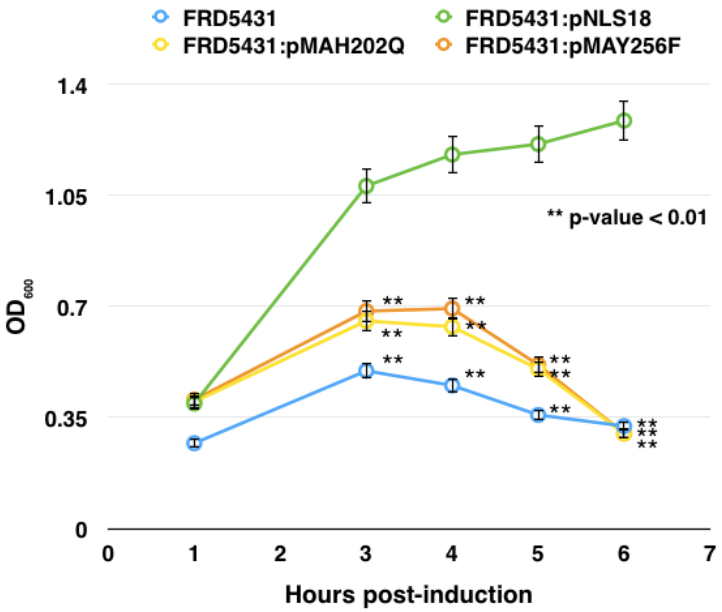

Figure 11. OD600 growth curve comparing the non-viable ΔalgL, FRD5431, to the various rescue strains containing either pNLS18, pMAH202Q or pMAY256F.

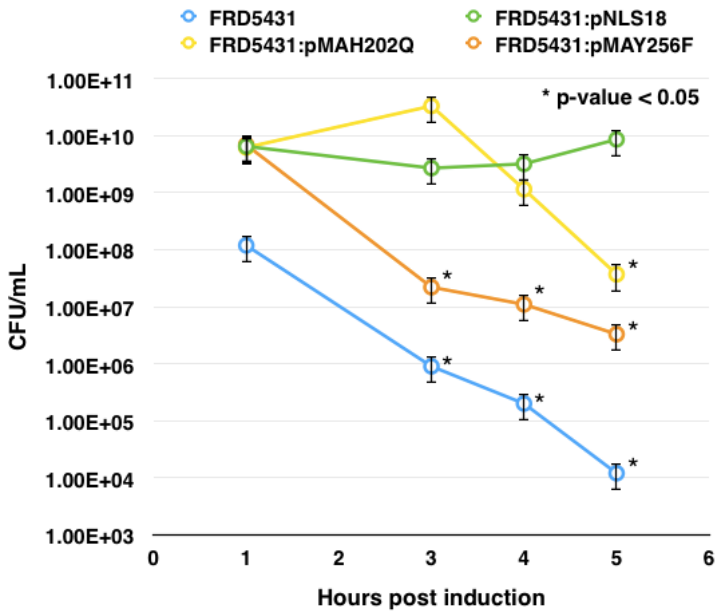

Figure 12. Viable cell counts comparing the non-viable ΔalgL, FRD5431, to the various rescue strains containing either pNLS18, pMAH202Q or pMAY256F. Values represent the average of at least three replica experiments.

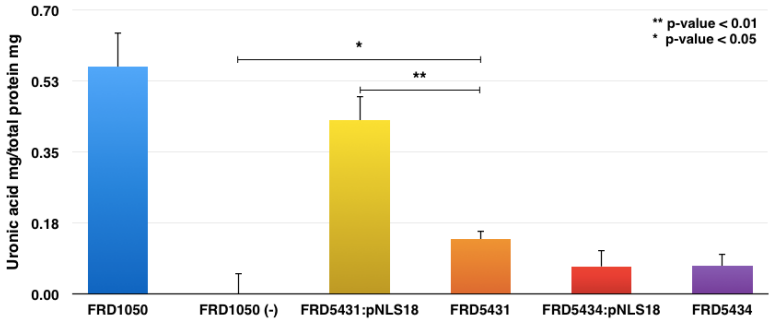

Figure 13. Uronic acid production of FRD5431 and FRD5434 rescued by pNLS18 compared to FRD1050 and FRD5431. Negative (-), uninduced culture. Values represent the average of at least three replica experiments.

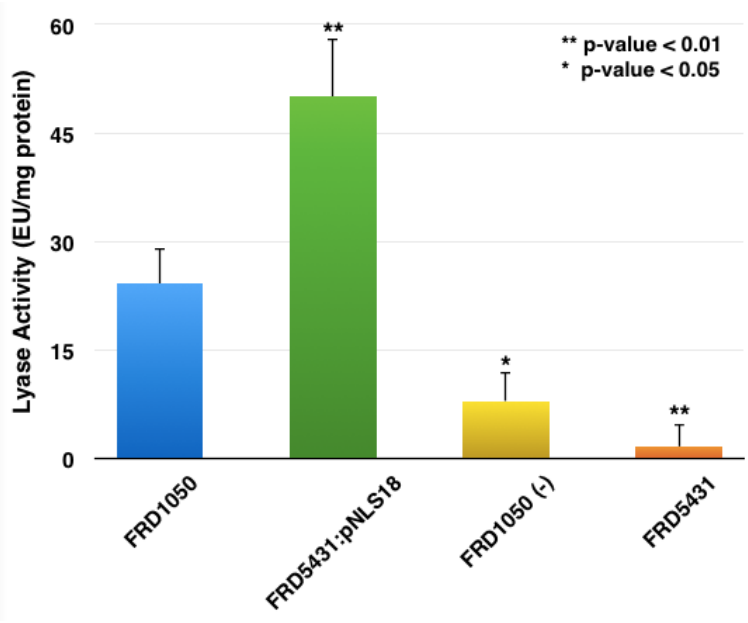

Figure 14. Lyase activity detected in FRD5431 compared to FRD1050 and FRD5431 rescued by pNLS18. negative (-), uninduced culture. Values represent the average of at least three replica experiments.

Transformation of pMAH202Q and pMAY256F into FRD5431 was achieved by triparental mating, as before with pNLS18. Colonies were confirmed using a three-primer scheme similar to the previously mentioned PCR screening approach differing only by primers. Primers A and B produced a 960 bp band amplifying the 5' end of *algL* through to the 3' end of the gentamicin cassette. Primers A and C produced a ~1600 bp product that begins at the 5' of *algL* and reads onto the pRK415 plasmid.

FRD5431 strains complemented with pNLS18, pMAH202Q or pMAY256F were grown in liquid culture as described above. Prior to induction, each strain grew normally, as expected. The strains were then induced with 0.5 mM IPTG during early log-phase. Similar to the previously observed growth pattern, FRD5431, FRD5431:pMAH202Q and FRD5431:pMAY256F were able to grow for 3 hours before a significant drop in OD_{600}

and viable cell count was observed (Figure 11 and 12). FRD5431:pNLS18, an *algL* knockout complemented with a catalytically active AlgL grew without problem over the length of the experiment. Samples from each culture were isolated after 16 hours induction. The total protein of each culture was determined by Bradford assay [133] and supernatants were used to determine uronic acid production. Lyase activity was determined by isolating a periplasmic protein from each culture at 3 hours. This time point was chosen because the optical density of each culture at that time was relatively close together. A significant ($p<0.001$) increase in uronic acid production in FRD5431 cultures expressing the AlgL H202Q or Y256F mutants was observed, (Figure 15); however, neither of the AlgL mutants expressed significant lyase activity, (Figure 16).

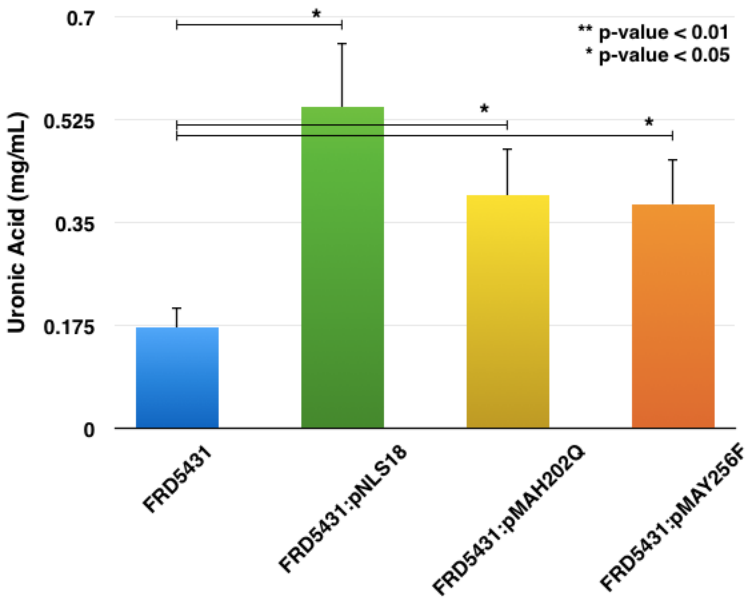

Figure 15. Uronic acid production from rescued FRD5431 strains. FRD5431 is compared to FRD5431 strains expressing AlgL from pNLS18, AlgLH202Q from pMAH202Q, and AlgLY256F from pMAY256F. Values represent the average of at least three replica experiments.

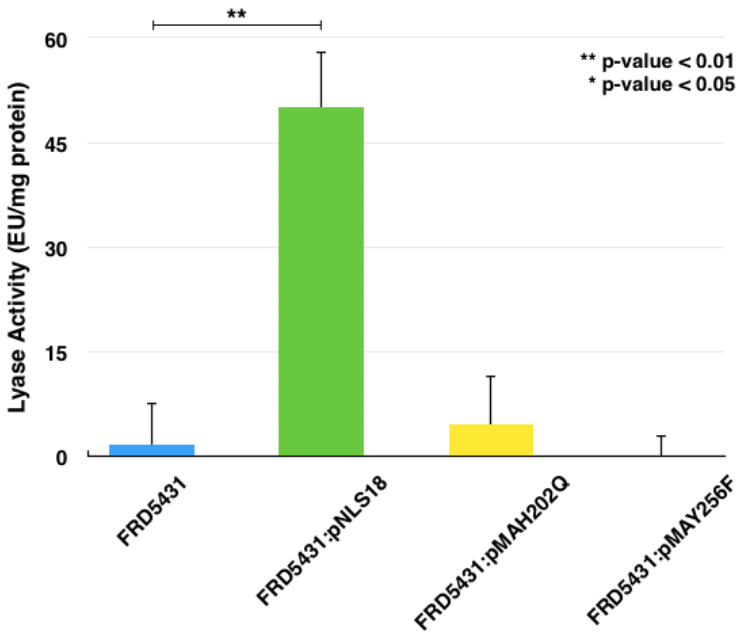

Figure 16. Lyase activity from rescued FRD5431 strains. FRD5431 is compared to FRD5431 strains expressing AlgL from pNLS18, AlgLH202Q from pMAH202Q, and AlgLY256F from pMAY256F. Values represent the average of at least three replica experiments.

AlgL-HA complementation, expression and Co-IP in FRD5431: Candidate colonies isolated from the triparental mating of pBLHA into FRD5431 were screened using the previously mentioned three-primer PCR protocol outlined earlier. As expected, two bands are plainly visible at 960 bp and 690 bp, representing the KO *algL* gene and the WT gene, respectively. Confirmed individual colonies were cultured on PIA Tc_{100} Gm_{50} supplemented with IPTG. Cultures were induced for 16-24 hours to confirm a mucoid phenotype. Induced transformants were visibly mucoid when compared to induced FRD1050 (data not shown), produced comparable uronic acid to FRD5431:pNLS18 (Figure 17), and were lyase positive (Figure 18). Confirmation of expression was achieved by western blot using HA specific epitope antibodies. Two bands, 46 kDa and 43 kDa, were visible in the insoluble extract. The 46 kDa MW band

corresponds to the AlgL-HA protein that still contains the signal localization peptide, which contributes ~ 3 kDa to the MW (Figure 19). This higher MW band is less abundant in the soluble extract that contains primarily periplasmic proteins, which have the signal sequence removed. DSS was used to crosslink concentrated sonicated extract in hopes of isolating protein-protein interactions. Protein G anti-HA conjugated Dynabeads® were subsequently used to immunoprecipitate (IP) crosslinked AlgL-HA. IP samples were then separated by SDS-PAGE and enrichment was detected by western blot using anti-HA IgG. AlgL-HA was successfully enriched in both DSS treated and untreated samples. Two additional, higher MW bands were detected in the DSS eluted sample, at ~60 kDa and at ~115 kDa (Figure 20). The band at ~60 kDa is also present in the untreated sample and, as such, is a non-specific interaction. However, the band at ~115 kDa is not present in the untreated sample and might represent an important protein-protein interaction.

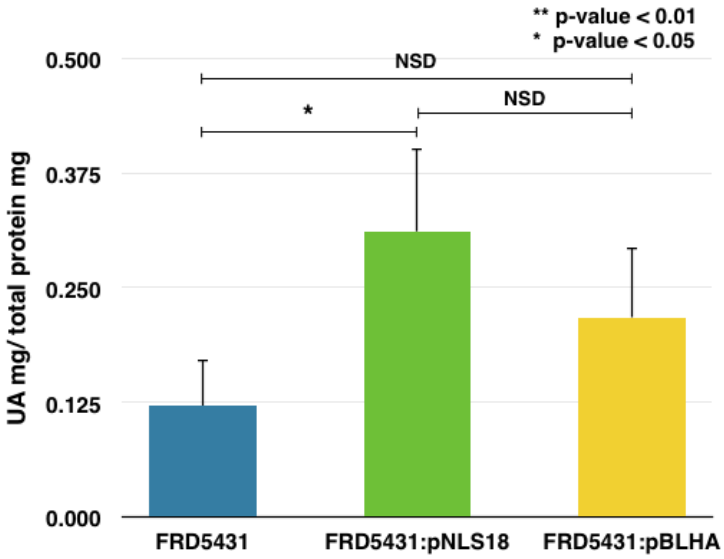

Figure 17. Uronic acid production from FRD5431:pBLHA compared to FRD5431:pNLS18 and FRD5431. Values represent the average of at least three replica experiments. NSD, not significant

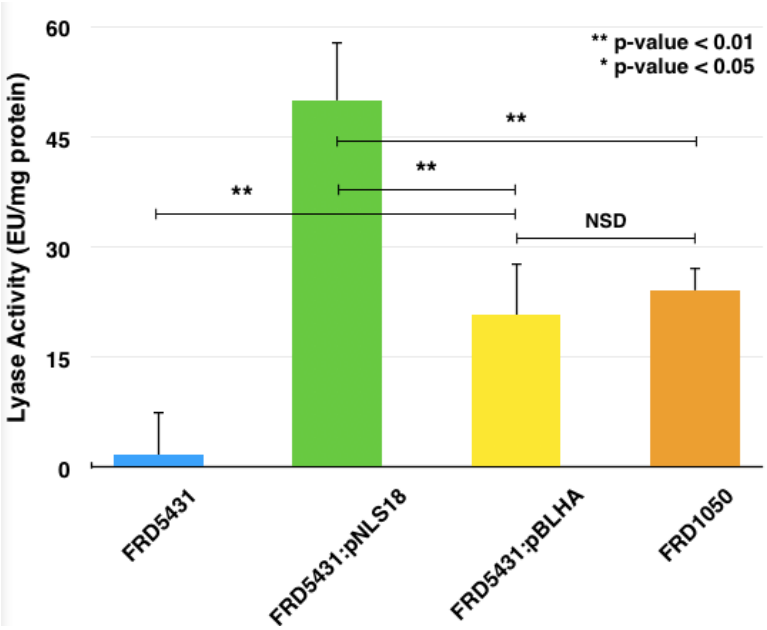

Figure 18. Lyase activity detected in FRD5431:pBLHA compared to FRD1050 and FRD5431:pNLS18. Values represent at least three replica experiments. NSD, not significant.

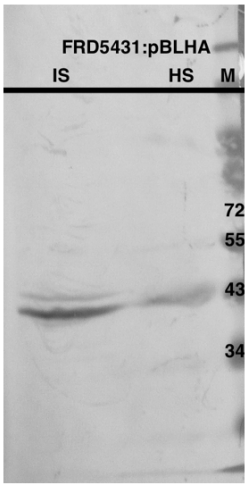

Figure 19. Western blot analysis of FRD5431:pBLHA. The insoluble sample (IS) contains two bands, presumably the cytoplasmic (~46kDa) and periplasmic protein (~43kDa). HS, or soluble sample, contains primarily the periplasmic protein.

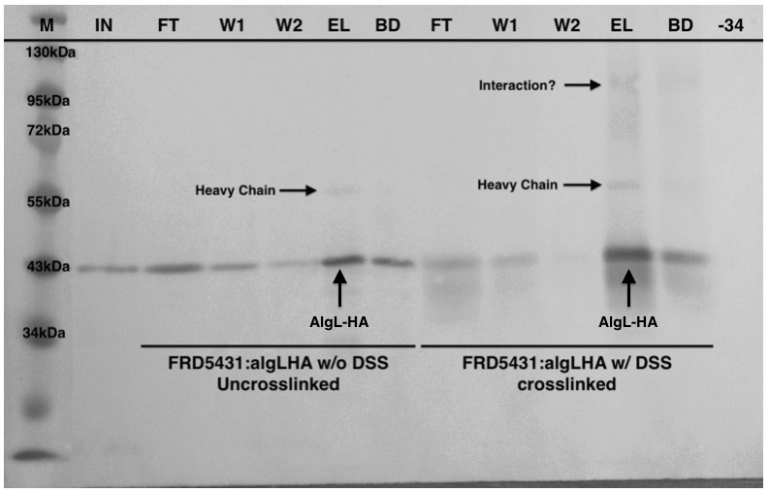

Figure 20. Immunoprecipitation of crosslinked and non-crosslinked AlgL-HA protein. There are higher MW bands at ~60 kDa and ~110 kDa. FT represents unbound flowthrough. W1 and W2 represent Wash samples. EL represents eluted proteins. BD represents residual bound protein on the beads.

2D-LC (MudPIT) Q-TOF mass spectroscopy: DSS treated and untreated eluted protein samples were provided to Dr. Songqin at IIGB. Following trypsin digests and MS analysis, a majority of identified peptides were either metabolic enzymes or transcription and translation factors (data not shown). Even worse, AlgL was only detected in the DSS treated sample and not in the untreated sample. There was enrichment of various proteins associated with alginate biosynthesis, such as AlgZ, AlgP, AlgC, and MucD (data not shown). However, AlgG, AlgX, or AlgK, the periplasmic components of alginate synthesis, were not detected in the DSS treated sample.

Discussion

Characterization of FRD1050Δ*algL* knockout phenotype with in-trans expression of AlgL: Previous attempts to make an *algL* knockout in a mucoid background such as FRD1 have been unsuccessful. There has been recent success

creating an *algL* knockout in an inducible background, FRD1050. This study has created the third published non-polar *algL* knockout in the FRD1050 background (FRD1050Δ*algL*). This was accomplished by allelic exchange, using a plasmid constructed in a previous study, pMA5. pMA5 was constructed in the pEX100T backbone, which was designed for allelic exchange experiments[123]. The exchange vector, pEX100T, lacks an origin of replication necessary for its replication in FRD1050. As a result, pMA5, which carries a gentamicin cassette in the ΔAlgL, must undergo a crossover with the genomic DNA of FRD1050; so that FRD1050 can gain resistance to gentamicin. The plasmid becomes integrated into the genome of FRD1050. The recombination of the plasmid with the genome can occur within the upstream *algG-algX* fragment of flanking DNA or in the downstream *algI-algF* flanking fragment. A recombination upstream of *algL* results in a strain of bacteria that is unable to produce alginate because the gentamicin promoter is not located close enough to the functional *algL-algA* gene region. On the other hand, a recombination downstream in *algI-algF* region, locates the promoter directly upstream of *algI-algA* genes and allows for expression, resulting in alginate production[40]. Therefore, mucoid merodiploid colonies ensure that the initial crossover occurred downstream of *algL* and locates the gentamicin promoter correctly upstream of *algI-algA*. Once integrated, the plasmid backbone can be selected against by inoculating the merodiploid on media containing sucrose. The expression of *sacB*, present on the pMA5 plasmid, is lethal to the bacteria in the presence of sucrose. As a result, FRD1050 merodiploid cells must undergo a second crossover, which kicks out the WT *algL* gene and the plasmid backbone, retaining the

algL KO and gentamicin cassette needed for resistance. Based on previous experiments, the expected phenotype of the *algL* KO was a viable mutant, which lacks a necessary protein, AlgL, to synthesize alginate. However, this expectation was incorrect, or at least partially incorrect, because three-quarters of the FRD1050Δ*algL* mutants isolated were not viable when induced. This population is represented by the FRD5431 strain, and is capable of synthesizing some uronic acid polymers, when induced. The remaining 25% of the isolated mutants were viable and non-mucoid. This population is represented by the FRD5434 strain. It was unclear which phenotype, FRD5434 or FRD5431, represented the correct phenotype for *algL* deletion mutant. The pivotal experiment was the recovery of the parent phenotype, viable and mucoid, by reintroducing a functional *algL* gene. This demonstrates that no other genes were impacted by the creation of the *algL* deletion mutant. Transformation of pNLS18 into FRD5434 was not able to rescue the parental mucoid phenotype. This might indicate that a secondary mutation occurred in FRD5434 and is responsible for the non-rescuable phenotype. Mutations in *algD, algA*, and *alg8* could prevent alginate production, however sequencing of *algD* and *algA* in FRD5434 did not identify any mutations. Attempts to sequence *alg8* were unsuccessful, possibly due to mutations in *alg8*. As for FRD5431, this strain was rescuable by expressing AlgL in-trans, recovering both viability and uronic acid production. This confirmed that the phenotype observed by Jain et al.[37] represents the true phenotype of a non-polar *algL* knockout.

Attempts to recover the FRD1050 phenotype with catalytically inactive AlgL: The previous rescue of FRD5431 demonstrated the necessity for AlgL to be

present in the periplasm during alginate biosynthesis. However, it still remained unclear whether AlgL is a component of a multi-protein complex (MPC), which aided the transportation and modification of alginate polymers through the periplasm. At this juncture there seemed to be three possible scenarios. First, AlgL could be a structural component of the multi-protein complex but not catalytically involved in any aspect of alginate synthesis. If true, in the presence of an inactive AlgL protein, alginate would still be synthesized and complementation would result in the parental phenotype. A second possibility is that AlgL is a component of the MPC and contributes, catalytically, to alginate biosynthesis, in some part, possibly by regulating polymer length. Opposed to the first scenario, the presence of catalytically inactive AlgL proteins would stall alginate synthesis. Complementation would result in a viable cell, which is unable to produce alginate. The third scenario would be that AlgL is not associated with the MPC and functions, enzymatically, to degrade alginate polymers that are erroneously shuttled to the periplasm. The expression of a catalytically inactive AlgL leaves the cell vulnerable to alginate polymers that are improperly localized to the periplasm. Similar to induced FRD5431, this accumulation would result in the lethal phenotype. Therefore, complementation by catalytically inactive AlgL site-directed mutants is capable of distinguishing between the need for AlgL lyase activity and the need for AlgL as a structural component.

FRD5431 maintaining pMAH202Q or pMAY256F were unable to grow on PIA supplemented with IPTG. However, FRD5431 expressing either mutant was able to produce a similar amount of uronic acid when compared to FRD5431:pNLS18. This

suggests that the presence of AlgL allows for synthesis to proceed though it does not prevent the accumulation of uronic acid in the periplasm. This observation was further characterized by growth curve and viable cell count experiments. FRD5431:pMAH202Q and FRD5431:pMAY256F exhibited decreased cell density and viable cell count after 3-4 hours of induction, similar to FRD5431, though not as drastic. Supernatant samples from each mutant rescue, H202Q and Y256F, produced comparable levels of uronic acid to the non-mutant rescue, pNLS18. The higher number of viable cells in the H202Q and Y256F rescue could account for the higher alginate production. Periplasmic protein extract from either complementation does not exhibit additional lyase activity, compared to FRD5431 and FRD5431:pNLS18.

Ultimately, expression of catalytically inactive AlgL proteins does not rescue viability in FRD5431. The marginal increase of alginate production could be accounted for by the presence of slightly more viable cells in the mutant cultures. The presence of a catalytically inactive AlgL does not replace the role of a functional AlgL with respect to alginate transport and potential interaction with the MPC. Inevitably, due to spontaneous disassembly or improper assembly of the periplasmic complex, alginate accumulates naturally in the periplasm, which, due to the lack of a functional alginate lyase, results in lysing of the bacterial cells as was observed by Jain et al.[37]

Detection of cross-linked protein-protein interactions by MS-MS: Identification of protein-protein interactions with AlgL was achieved by utilizing an epitope tagged AlgL expression construct within FRD5431. The epitope tag had to be added to the C-terminal end of the protein due to a signal sequence at the N-terminal

end of the protein, which is essential for proper localization to the periplasm. Whole cell sonicated extracts were isolated from FRD5431:pBLHA strain. The whole cell extract was split; half was treated with disuccinimidyl suberate (DSS), while the other half remained untreated. DSS is a molecular cross-linker with an 8-atom arm (11.4Å), which reacts with primary amines present on lysine residues and at the N-terminal of peptides. AlgL contains 22 possible reactive sites, 21 lysines and the N-terminus. Cross-linked samples were enriched by immunoprecipitation using rabbit anti-HA IgG conjugated to protein G Dynabeads® and were confirmed by western blot. Eluted protein mixtures were analyzed by 2D-LC (MudPIT) Q-TOF mass spectroscopy. A majority of proteins identified in either sample, DSS-treated or untreated, were transcription factors, translation factors or metabolic enzymes. This suggests that a significant amount of protein is interacting with the beads non-specifically and further washes might be needed to completely remove these contaminants. Comparison of identified proteins within enriched DSS treated and untreated samples indicate slightly higher relative concentrations of various alginate biosynthesis associated proteins, AlgP, AlgZ, and MucD. While the enrichment of these proteins might suggest an interaction, both AlgP and AlgZ are present within the cytoplasm and are involved in gene expression. Enrichment of MucD is an interesting target because it has previously been co-purified with AlgX[134], though it's involvement with AlgX still remains uncertain. In addition, the 115 kDa MW band detected on the western blot is relatively close to the combined MW for MucD and AlgL, ~ 93 kDa. AlgL was only detectable in the DSS treated sample. This might be caused by a low concentration of AlgL in the untreated sample, significantly

lower than expected. If concentration is an issue, it could be compounded by trypsin digest of AlgL producing too few analyzable peptides (20-30 residues). AlgL contains 21 lysines and 12 arginine cleavage sites; combined full digest only produces a few fragments within the desired range.

In conclusion, all of these results suggest that AlgL is a lone wolf protein scavenging for stray alginate polymers within the periplasm. Mass spectroscopy analysis revealed no additional information supporting any novel protein-protein interaction. So AlgL is not a component of a multi-protein biosynthesis scaffold required for alginate biosynthesis. AlgL is required for cell viability to protect against mis-guided alginate polymers that enter the periplasm. Thus, these findings support the role for AlgL suggested by Jain et al.[37]

Chapter 4 - Characterization of the C-terminal carbohydrate-binding domain in AlgX.

Abstract

Alginate encapsulated *Pseudomonas aeruginosa* is the primary causative agent of respiratory insufficiency and failure in patients with cystic fibrosis (CF). AlgX is a protein that is required for alginate biosynthesis and has been suggested to participate in alginate acetylation. We demonstrated that in the absence of AlgX, 100% of uronic acid polymers produced by the *algX*-deleted mutant are subsequently degraded by AlgL, an alginate lyase that is responsible for cleaving misguided alginate polymers. Using alginate affinity assays and molecular docking studies, we demonstrated that AlgX binds alginate via the carbohydrate-binding module (CBM) located in the C-terminal region of AlgX. Alanine mutations of the predicted amino acid residues that interact with alginate suggest that Arg-338, Lys-370, Thr-372, and Arg-380 are important for alginate binding. Alginate rescue assay by *in trans* expression of mutant AlgX in the *algX*-deleted mutant confirms the importance of the CBM domain. These observations suggest that AlgX binds alginate via the CBM domain and this is important for alginate biosynthesis in *P. aeruginosa*.

Introduction

Cystic fibrosis (CF) is the most common life-shortening genetic inherited disease in Caucasians. According to the Cystic Fibrosis Foundation, the suggested median survival age of CF patients is 36.8 years[135]. *Pseudomonas aeruginosa* is a gram negative, opportunistic pathogen, which is found throughout the environment. Since the introduction of anti-staphylococcal drugs, *P. aeruginosa* has become the predominant bacterial infection in individuals suffering from cystic fibrosis (CF). Cystic fibrosis transmembrane conductance regulator (CFTR) is a regulated chloride channel which is localized to the apical surface of epithelial cells[6]. The disease impacts secretions from the gastrointestinal tract, the pancreas, and even the male reproductive tract; however, the most significant impact is on the lungs[10]. Mutations in CFTR lead to improper fluid transportation and the build-up of thick mucus in the lungs[6]. The altered lung environment allows for the colonization of various bacteria, most importantly *P. aeruginosa*. Infections start in early childhood and over time, due to re-infection, develop into chronic infections that are difficult to eradicate[10]. Progression to a chronic infection is concurrent with *P. aeruginosa*'s constitutive production of alginate. Alginate is an exopolysaccharide, which forms a protective barrier around the bacteria, protecting from host immune responses and chemical therapeutics.

Production of alginate is achieved by expression of the twelve-gene alginate biosynthetic operon (*algD-algA*) and a single separately expressed gene (*algC*). Biosynthesis of alginate begins with the conversion of fructose-6-phosphate to GDP-mannuronic acid in 4 steps. Two reactions are catalyzed by AlgA, one by AlgC and AlgD.

Alg8, functioning in concert with Alg44, then polymerizes the GDP-mannuronic acid into a mannuronic acid polymer (Alginate). The polymer is passed through the inner membrane into the periplasm. It remains unclear how the polymer eventually reaches the outer membrane and becomes secreted from the cell by AlgE, an outer membrane porin protein. However, it is speculated that a multi-protein complex (MPC), consisting of AlgK-AlgG-AlgX, transports the polymer through the periplasm and protects the polymer from alginate lyase (AlgL) degradation. At the same time, AlgG is responsible for intermittently epimerizing mannuronic acids into guluronic acids. As well, a second complex consisting of AlgF-AlgI-AlgJ, and possibly AlgX, sporadically acetylates mannuronic acids within the polymer.

AlgX was recently crystallized by Weadge et al.[136]. Those crystals were used by Riley et al. to determine the protein structure[49]. Structural analysis identified two distinct domains, a N-terminal SGNH hydrolase-like domain, and a C-terminal putative carbohydrate-binding module (CBM). This recent study also examined the potential for AlgX's role in mannuronic acid acetylation. In addition to identifying the structure of AlgX, they also examined various N-terminal mutations and their impact on acetylation. The study successfully identified three residues, Ser 269, Asp 174, and His 176, which are critical to mannuronic acid acetylation. Characterization of the C-terminal domains was limited to homology modeling and speculation of a type B CBM. The CBM is thought to be composed of a solvent exposed Trp 400 and local polar residues, Arg 364, Thr 398, and Arg 406, which form a "pinch point" for carbohydrate binding. Two additional Lys residues at 396 and 410 were predicted to guide the polymer along the surface of the

protein. However, further examination of these residues was not performed and the role they play in alginate binding remained speculative.

Methods and Materials

Computational polysaccharide docking: Computational analysis was performed in collaboration with the Morikis Laboratory and Zied Gaieb. Starting with the crystal structure of AlgX (code 4KNC), provided by the Protein Data Bank (PDB) and originally obtained by Riley et al., a complete structure of AlgX was generated. This was accomplished using molecule B from the PDB file. The file contains the crystal structure of two AlgX molecules, a dimer, of which, molecule B was the most complete, and was extracted for further analysis. To fill in gaps caused by poor electron density, the complete AlgX sequence, obtained from UNIProt was modeled to Molecule B using Modeller, generating a complete AlgX structure. The structure generated lacks the N-terminal signal sequences; regardless, amino acids are numbered to include the signal peptide.

Computational docking using Autodock Vina v1.1 has previously been successful at predicting confirmation preference and free energy binding[137]. Therefore, Autodock Vina was used to determine the docking of 11 different generated mannuronic and guluronic acid polymers, which included acetylation and reduced ends, to the generated structure above. The structure of uronic acid monomers was previously determined (PDB code 2PYH, 1HV6, and 1Y3P)[44, 138, 139] and utilized to create various polymers for this study. AutoDockTools was used to prepare the ligand and AlgX

structure for docking by adding polar hydrogens to both, as well as setting the ligand bonds as rotatable; this produced two pdbqt files.

Docking was restricted to the C-terminal carbohydrate-binding module (CBM) located within a grid box of 27.5 x 41.75 x 34.3 Å[140]. Autodock Vina was used to generate 20 docking models between each of the various polysaccharides and defined docking region with an exhaustiveness of 100 for increased search accuracy. Models that docked the polysaccharide within the pinch point were chosen for further analysis by a custom script written with Bio3D v2.0 R package along with UCFS chimera v1.8.1. The script determined the frequency of H-bonds, charged-charged (<5 Å between charged groups) and dipole-dipole interactions between AlgX residues and the docked polysaccharide.

Creating the complementation vector pUCP21T:*algXHis*: The creation of pUCP21T:*algXHis* was achieved initially by PCR amplification of the *algX* open reading frame from FRD1050 genomic DNA. The PCR was performed using the forward primer, 5'AAA AAA AGC TCT AGA GAT GAA AAC CCG CAC TTC CCG (*XbaI+algX*), which introduces a XbaI restriction site, and the reverse primer, 5'CGC CGC GGA TCC TTA GTG GTG ATG GTG ATG ATG CTT AAG CCT CCC GGC CAC CGA CTG GCT (-*algXHis6*), which introduces a hexahistidine epitope tag, as well as, a *Bam*HI restriction site; complementary regions are underlined. Primers were created by Integrated DNA technology (IDT). The PCR was performed on ~100 ng FRD1050 genomic DNA with 0.2 µM of each primer, 3% dimethyl sulfoxide (DMSO), and Apex Taq Mastermix (Genesee Scientific). An aliquot of PCR reaction was confirmed by electrophoresis on a 1%

agarose gel made with 89 mM pH 8.3 Tris buffer supplemented with 89 mM borate and 2 mM EDTA (TBE). Ethidium bromide was added to the gel, at 0.5 µg/mL, prior to the gel solidification, to allow detection of the migrated DNA.

Once confirmed, the remainder of the reaction was purified by PCR purification kit (Promega). The purified PCR reaction was then double digested, overnight at 37°C, using *Xba*I (New England Biolabs) and *Bam*HI (New England Biolabs), following manufacturer's specifications. Roughly 1 mg pUCP21T plasmid was digested at the same time using the identical protocol. The digested PCR product and plasmid were subsequently purified using PCR purification kit (Promega) and ligated together using T4 Ligase (New England Biolabs), following manufacturer's specifications. The resulting product was then transformed into *E. coli* GeneHog® (Invitrogen) cells that were prepared following a previously established protocol[128]. A 100 µL aliquot of electrocompetent cells was combined with 4-5 µL ligation reaction in a 2 mm gap electroporation cuvette. The mixture was incubated on ice for 10 minutes prior to electroporation at 2.5 kV, 150 Ω, and 25 µF. Electroporated cells were resuspended in 400 µL SOC media (Sigma Aldrich) and recovered for 1 hour at 37°C with agitation before plating on Luria Agar (LA) supplemented with 50 µg/mL tetracycline (Tc_{50}), 1 mM isopropyl beta-D-thiogalactopyranoside (IPTG) and 40 µg/mL 5-bromo-4-chloro-3-indolyl-beta-D-galactopyranoside (X-gal) for 16-24 hours in a 37°C humidified incubator.

White colonies were isolated and screened by PCR. Briefly, an individual colony was resuspended in 3% DMSO with 0.3 µM forward and reverse primers, 5'-GCG CGT

CGG CCT GCT GTC CA (*algX +630*) and 5'-GCC TCT TCG CTA TTA CGC CA (*MCS* -), respectively, and 2x Apex Taq Mastermix. Again, an aliquot of each reaction was confirmed by gel electrophoresis on a 1% TBE gel. The remaining PCR product was purified, as before, and sequenced at the University of California at Riverside Institute for Integrative Genome Biology (IIGB) using the forward primer *algX +630*.

Site-directed mutagenesis of complementation vector pUCP21T:*algXHis*: Site-directed mutagenesis of pUCP21T:*algXHis* was achieved using the Q5® site-directed mutagenesis kit (New England Biolabs). The mutations were introduced by PCR amplification, as directed by the manufacturer, using the primer pairs generated by the NEBaseChange™: *R364A+Q5SDM* (5'-GCG CCA GGG CGC CAA CGA GGT GC), *R364A-Q5SDM* (5'-AGC TTG ACC TTG CGG CTG), *K396A+Q5SDM* (5'-ACA CGA GTT GGC GAA CAC CAT CTG GTA C), *K396A-Q5SDM* (5'-ACC GAA GGG TCG CTG TAG), *T398A+Q5SDM* (5'-GTT GAA GAA CGC CAT CTG GTA CAT G), *T398A-Q5SDM* (5'-TCG TGT ACC GAA GGG TCG), *W400A+Q5SDM* (5'-GAA CAC CAT CGC GTA CAT GAA CGG CC), *W400A-Q5SDM* (5'-TTC AAC TCG TGT ACC GAA G), *R406A+Q5SDM* (5'-GAA CGG CCG CGC CGA GCA GTT G), *R406A-Q5SDM* (5'-ATG TAC CAG ATG GTG TTC), *K410A+Q5SDM* (5'-CGA GCA GTT GGC GAT CGA GCA GTC GAA AG), and *K410A-Q5SDM* (5'-CGG CGG CCG TTC ATG TAC); all primers were ordered from Integrate DNA Technologies (IDT); underlined sequences represent complementary regions. The PCR reactions were carried out following the recommended manufacturer's protocol and specifications. The resulting PCR products were treated with the provided

KLD enzyme mixture and transformed into chemicompetent NEB 5α cells, also provided by the manufacturer. The transformation was then selected on LA Tc_{50} overnight at 37°C in a humidified incubator. Individual colonies were screened using the previously mentioned PCR screening protocol and subsequently sequenced, with *algX +630*, to confirm mutagenesis at the IIGB.

Transformation of complementation vectors into FRD1050Δ*algX*: Vectors created in this study were transformed into FRD1050Δ*algX* to assess their capacity to recover large polymer uronic acid production equivalent to that of the parent strain, FRD1050. Plasmids were purified from confirmed transformants in GeneHog® (pUCP21T:*algXHis*) and NEB 5α (Site-directed mutants) by Zyppy™ Plasmid miniprep Kit (Zymo Research). Electrocompetent cells were prepared following the previously published protocol by Diver et al[141]. An aliquot of prepared electrocompetent cells was combined with 200 ng purified plasmid and incubated on ice for 10 minutes, followed by electroporation at 2.5 kV, 250 Ω, and 25 μF. Cells were resuspended in 400 μL SOC media (Sigma Aldrich) and recovered for 1 hour at 37°C with agitation. Recovered cells were selected on *Pseudomonas* Isolation Agar (PIA) with 100 μg/ml tetracycline (Tc_{100}) and 50 μg/ml gentamicin (Gm_{50}). Complementation colonies were screened using PCR following the colony screening protocol discussed above.

Characterization of complementation phenotype: Uronic acid quantification was accomplished using the previously established protocol by Knutson et al.[126]. Confirmed complementations expressing AlgX-His or any of the six mutated AlgX-His

proteins, were plated on PIA Tc_{100} Gm_{50}, and induced by spreading 50 µL 0.5M IPTG onto the plate prior to inoculation. Plates were incubated for 16-24 hours before cells were scraped from the plates and resuspended in 1mL Tris Buffered Saline, 50 mM Tris-Cl, 150 mM NaCl at pH 7.5 (TBS). Cells were separated by centrifugation at 16,783 x g for 5 minutes at 4°C, and the supernatant was collected. To distinguish between large polymer uronic acid (> 30 kDa) and small polymer uronic acid (< 30 kDa), supernatant aliquots were passed through a 30 kDa MWCO Amicon® Ultra-15 centrifugal filter (Millipore) by centrifugation at 4842 x g for 10 minutes at 4°C. The uronic acid concentrations in flow-through and unfiltered samples were determined for each complementation using the 30 minute at 55°C protocol established by Knutson[126]. Expression of AlgX was determined by western blot using polyclonal rabbit α-His IgG (Cell Signaling). Western blot protocol was adopted from Gallagher[129].

Expression and isolation of AlgX: To improve the level of protein expression, the pUCP21T:*algXHis* vector along with the pUCP21T:*algXHis* site-directed mutants were transformed into *E. coli* BL21(pLys)DE3 cells using the transformation protocol for *E. coli* described above. Transformants were selected on LA Tc_{50} overnight in a 37°C humidified incubator. Colonies were confirmed using the previously described colony screening PCR protocol.

An individual, confirmed colony was used to inoculate a 2 mL Luria Broth (LB) Tc_{25} culture. The culture was grown overnight at 37°C with agitation. The resulting culture was used to inoculate a 250 mL LB Tc_{25} culture, which was grown under the

same conditions to an optical density of 0.7-0.8 at 595nm (OD_{595}). At this point the culture was induced by adding IPTG to 0.5 mM. The culture was grown for an additional 12-16 hours. At that time the cells were isolated by centrifugation at 8,240 x g for 15 minutes at 4°C. Cells were washed three times with cold TBS and resuspended at a concentration of 100 mg wet cell weight per 1 mL buffer. Cells were resuspended in TBS supplemented with 1 mM dithiothreitol (DTT), 1 mM phenylmethanesulfonyl fluoride (PMSF), 200 µg/mL of lysozyme, and 3% v/v glycerol. The cell mixture was allowed to incubate at 4°C for 2-3 hours then subjected to 3 cycles of sonication for 15 seconds each at 50% duty. Residual cellular debris was removed by centrifugation at 12,900 x g for 20 minutes at 4°C. The supernatant was collected and filter sterilized using a 0.45 µm-pore-size syringe filter (Millipore).

The enrichment of AlgXHis and mutated AlgXHis (AlgXHis*) was accomplished using Ni-NTA His-Bind® resin (Novagen). Initially, the Ni-NTA His-Bind® slurry was equilibrated using TBS supplemented with 200 mM KCl, 1 mM imidazole and 1 mM β-mercaptoethanol (Binding buffer) at 1:4 v/v ratio. The resin was allowed to settle, which permitted the removal of the supernatant and replacement by an equal volume of AlgXHis(*) sonicated protein extract. The protein-resin mixture was incubated at 4°C for 2 hours with gentle agitation, allowing for resin binding. Following this incubation period, the mixture was added to a chromatography column and was emptied by gravity at room temperature (24-27°C) at ~50 µL per second. The packed column was subsequently washed twice with 4 mL TBS supplemented with 200 mM KCl, 1 mM β-mercaptoethanol,

and 20 mM imidazole and emptied as before; flow-through fractions were collected. Elution was accomplished by addition of 1 mL TBS supplemented with 200 mM KCl, 1 mM β-mercaptoethanol, and 200 mM imidazole to the column followed by emptying at ~50 µL per second; flow-through was collected. Successful enrichment was determined by western blot analysis using polyclonal rabbit α-His IgG.

Conjugation of alginate to sepharose beads and AlgX alginate binding assay: To assess the ability of AlgX to bind alginate, this study conjugated alginate from FRD1050 to EAH Sepharose 4B beads (GE Healthcare) using the crosslinking agent 1-ethyl-3-[3-dimethylaminopropyl]carbodiimide hydrochloride, EDC (Pierce Biotechnology). Alginate was purified from FRD1050 supernatant following the previously described protocol by Pedersen et al.[142]. Precipitated alginate was resuspended in 25 mM pH 4.5 HEPES buffer to a concentration of 30 µg/mL. The purified alginate was combined 1:1 with a 4 mL aliquot of sepharose beads that were previously washed three times with 10 mL pH 4.5 deionized water and resuspended in 10 mL pH 4.5 deionized water supplemented with 500 mM NaCl. This mixture was combined, drop-wise, with 2 mL 25 mM HEPES supplemented with 1 M EDC and allowed to incubate with agitation at 4°C for 2 hours. The reaction forms urea as a by-product of crosslinking, which shifts the pH. To avoid pH changes, the pH of the reaction was monitored throughout the 2 hours and adjusted, using 1 M solutions of either HCl or NaOH, to maintain a pH between 4-5. The conjugated beads were isolated by centrifugation at 3,200 x g at 4°C for 30 minutes and washed with 25 mM pH 7.6 Tris buffer. The conjugation of alginate to the beads was confirmed using the carbazole assay[126].

To assess the binding capacity of AlgXHis(*), a 0.7 x 5.5 cm chromatography column (Biorad) was packed with either unconjugated sepharose beads or alginate conjugated beads to a bed height of 1.50-1.75 cm. A 0.75 mL aliquot of enriched AlgXHis(*) protein extract was added to both columns and allowed to empty by gravity at ~50 µL per second. Columns were subsequently washed three times with an equal volume of 25 mM pH 7.6 Tris buffer. Elution of bound protein was accomplished by resuspending the beads in 0.75 mL 25 mM Tris buffer supplemented with 0.1% v/v β-mercaptoethanol followed by incubation at 100°C for 30 minutes. Supernatant was isolated by centrifugation at 2,000 x g for 15 minutes at 4°C. Flow-through samples were isolated at each step for western blot analysis, as previously described[129].

To quantitate binding, nitrocellulose blots developed with BCIP/NBT (PerkinElmer) were digitally recorded using an 8-megapixel-iSight camera. Images were converted to an 8-bit format in ImageJ 1.47v. Density was determined as average band intensity multiplied by band area and was converted to a percentage relative to AlgXHis(*) input.

Results

Alginate docking to the CBM of AlgX: The docking of various uronic acid oligomers to the CBM of AlgX identified amino acid residues that putatively interact with the oligomer[49]. A total of 96 models were assessed using the custom script and chimera (See Materials and Methods), which identified molecular interaction with neighboring amino acid residues. Of the amino acids characterized during the docking studies, six amino acids (R364, K396, T398, W400, R406, and K410) were also

suggested by Riley et al.[49] to be involved in uronic acid polymer binding. In general, oligomers that contained a mixture of mannuronic and guluronic acids were less sterically restricted and formed more bonds with the AlgX CBM. Acetylation did not significantly impact oligomer docking. K396, R406, K410 and E444 frequently formed charged-charged interactions with the docked oligomers, 100%, 57%, 76% and 49%, respectively (Table 4). Predictably, uncharged residues Q362, T398, Q408 and W400 did not form charged-charged interactions with the docked oligomers. The frequency of hydrogen bond formation was less predictable; nevertheless, K396, R406, and K410 again formed H-bonds very frequently, 100%, 95% and 94%, respectively (Table 4). Less frequency was observed with Q362 that formed bonds in 81% of the models. R364, Q408, E444, and D448 formed H-bonds more seldom, 33%, 66%, 39%, and 42%, respectively (Table 4). With exception to T398, differences in dipole-dipole interactions, which occur between all molecules, were less dramatic. Of the top residues, most formed dipole bonds with the oligomer in 34-51% of the models. T398 only formed dipole bonds in 6% of the models, compared to R364, E444 and E447, which formed dipole bonds in 87%, 93%, and 67%, respectively (Table 4). Overall, K396, R406, K410 and E444 are predicted to interact the most frequently with the docked oligomer, whereas, T398 and W400 are predicted to form the fewest interactions with the docked oligomers.

Calculated percent frequency of interaction			
Residue	H-bond	Charged-Charged	Dipole-Dipole
Q362	81%	0%	51%
R364	33%	32%	87%
K396	100%	100%	34%
T398	17%	0%	6%
W400	6%	0%	51%
R406	95%	57%	46%
Q408	66%	0%	42%
K410	94%	76%	34%
E444	39%	49%	93%
E447	3%	35%	67%
D448	42%	3%	37%

Table 4. Interaction frequency between docked uronic oligomers and carbohydrate binding module (CBM). Values represent the percentage frequency of various interactions between the oligomer and CBM in 96 analyzed models. Green, likely to interact with polymer. Red, unlikely to interact with polymer. White, unpredictable interaction with polymer

AlgX binding to alginate and the impact of CBM site-directed mutagenesis on alginate binding: To empirically determine that AlgX binds alginate and to characterize the contribution of individual residues within the putative CBM to alginate binding, this study utilized affinity chromatography. Immobilized, purified alginate was used as molecular bait for enriched AlgXHis and a variety of AlgXHis* (AlgX bearing amino acid mutations). Chromatography columns packed with alginate conjugated sepharose bead retained significantly more AlgXHis, 50.4±11.0% of input, compared to 16.3±3.5% of input retained by columns packed with unconjugated beads (null) (Figure 21). Site-directed mutations at R364, K396, T398, W400, R406 and K410 were made to investigate the CBM predicted by Riley et al.[49]. Alanine mutations at W400 and K410 had no impact on AlgXHis binding capacity to alginate, binding at 66.9±14.6% and 50.0±10.9% of input, respectively (Figure 21). On the other hand, alanine mutations at

R364 and K396 caused a marginal decrease in AlgXHis retention, 39.3±8.6% and 32.5±7.1% of input, respectively (Figure 21). Alanine mutations at T398 and R406 impacted retention significantly, reducing binding to 0.0±0.0% and 11.5±2.5% of input, respectively (Figure 21).

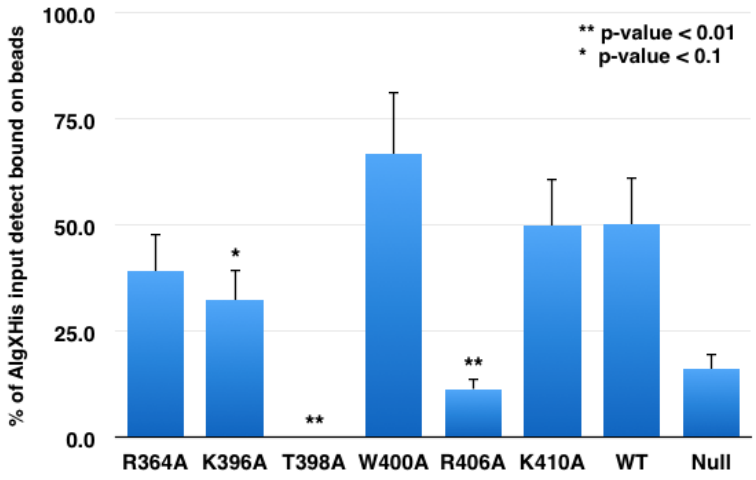

Figure 21. AlgXHis binding assay with various alanine mutants. Values represent the percent of protein retained by the column compared to the input. Percentages are an average of at least three replica experiments. Null, AlgXHis retained by non-alginate conjugated beads.

Complementation of FRD1050Δ*algX* by site-directed mutants: To assess the in vivo impact of site-directed mutagenesis on alginate production, plasmids carrying the alanine mutations at R364, K396, T398, W400, R406 and K410 were transformed into FRD1050*ΔalgX.* A previous study demonstrated that the lack of AlgX in FRD1050 produced a non-mucoid phenotype, which secreted 24% large polymer uronic acid (> 1 kDa)[39]. Complementation of FRD1050Δ*algX* by AlgXHis increases large polymer secretion to 72.4±0.7% (Figure 22). A similar phenotype was observed in

FRD1050Δ*algX* strains complemented by R364A, K396A, and K410A AlgXHis mutants, 80.0±18.8%, 75.6±0.9%, and 73.2±0.9%, respectively (Figure 22). Complementation by R406A AlgXHis mutant results in only 39.8±22.1% large polymer secretion compared to the AlgXHis complementation (low p-value due to high standard deviation). In contrast complementation by T398A and W400A AlgXHis mutants produce 42.1±9.0% and 30.7±2.1% large polymers, respectively, significantly less than the AlgXHis complementation (Figure 22).

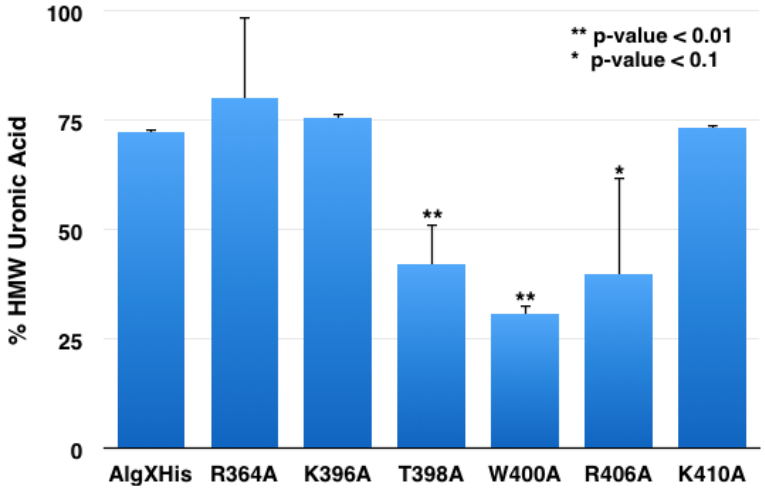

Figure 22. Measurement of large polymer uronic acid (> 30kDa) production by AlgXHis and various site-directed mutants. Values represent the average of at least three replica experiments.

Discussion

Docking studies identify statistically significant CBM residues: The goal of this docking analysis was to verify the speculations outlined by Riley et al.[49] and identify other residues essential to alginate binding. Riley et al. suggested that two polar residues, R406 and R364, together with an aromatic residue, W400, formed a “pinch point” for alginate binding. Inside the “pinch point”, an exposed R406 is suspected to aid

binding. Outside the “pinch point”, K396 and K410 were thought to direct the polymer across the protein surface. This study docked a combination of mannuronic and guluronic oligomers, with and without acetylation, to the CBM using AutoDock Vina. This allowed us to explore any polymer preference exerted by AlgX. Acetylated oligomers were not predicted to form significantly more or stronger bonds than those without acetylation. However, hetero oligomers consisting of both mannuronic and guluronic acid formed more flexible structures than strictly homo mannuronic or guluronic oligomers and as a result, were predicted to fit into and form more bonds with the CBM. This observation suggests that AlgX binding to the periplasmic alginate chain would occur after epimerization by AlgG.

This docking study identified K396, R406, and K410 as three residues with a high likelihood to interact with docked oligomers. Based on this docking study, K396 and K410 might play a more significant role in binding than previously thought. R406 likely functions in the “pinch point” role previously suggested; R364 was predicted to form fewer bonds and seems less probable. Previously, W400 was speculated to π-stack with the carbon ring of the polymer. However, this docking study suggests that W400 forms few bonds with the docked oligomers, suggesting that it plays only a minor role in binding. Similarly, this docking study suggests that R398 forms few bonds with the docked oligomer. The docking analysis identified two additional residues, Q362 and Q408, not previously mentioned[49], that could play a role in oligomer binding, most likely through H-bond and dipole-dipole interactions.

Site-directed mutagenesis of AlgXHis and the impact on AlgXHis function: Site-directed mutagenesis of residues within the CBM allows for directed analysis of individual amino acids and their contribution to alginate binding. This study attempted to identify the contribution of six amino acids identified by Riley et al.[49]. Investigation of binding was achieved by affinity chromatography, using immobilized alginate as bait for AlgXHis. Alanine mutations in AlgXHis at R364, K396, or K410 do not have a significant ($p > 0.19$) impact on alginate binding, compared to WT AlgXHis. Oddly, an alanine mutation at W400 dramatically increases the binding affinity of AlgXHis to alginate. AlgXHis W400A wash samples from alginate-conjugated beads contained 0.7±0.2% of input compared to an average of 16.7±3.6% of input in washes from all other samples (data not shown). On the other hand, FRD1050Δ*algX* rescued by AlgXHis W400A mutants were unable to recover synthesis of large alginate polymers. Speculatively, the alanine substitution at W400 could decrease the K_d of alginate and prevent the polymer from passing through the periplasm. This could block the synthetic machinery and due to spontaneous dissociation of the scaffolding complex, lead to alginate degradation by AlgL. The expression of R364A or K410A mutant AlgXHis in FRD1050Δ*algX* is able to recover the large alginate polymer synthesis, compared to AlgXHis. This empirically demonstrates that neither amino acid is essential to AlgX function within *P. aeruginosa*.

Expression of AlgXHis K396A in FRD1050Δ*algX* has a borderline significant ($p < 0.1$) impact on alginate binding. This same mutant is able to recover large alginate polymer synthesis in *algX* knockouts. Together, these findings suggest that K396 is not essential to AlgX function and alginate is able to bind or be directed across the protein

surface in the absence of K396. In contrast, expression of AlgXHis T398A or R406A in FRD1050Δ*algX* significantly ($p < 0.01$) decreases the binding capacity of AlgX. The T398A mutation resulted in no detectable bound AlgXHis in the affinity chromatography experiments, the most dramatic phenotype observed. These findings are strengthened by the lack of large alginate polymer synthesis in FRD1050Δ*algX* strains expressing either T398A or R406A mutant. The surface exposed T398 seems to play a significant role in alginate binding, even though the docking study suggested otherwise. Speculatively, T398 H-bonds with the bound alginate polymer, an interaction not possible by the alanine mutant. Based on the location of R406, it is likely the polar group forms one side of the alginate polymer "pinch point" binding site, an essential mechanism for alginate binding.

In conclusion, this study has identified two residues, T398 and R406, which are located in the C-terminal carbohydrate-binding module (CBM) that are critical to alginate binding and essential for AlgX function within the periplasm. Other residues identified by the AutoDock Vina docking study, such as Q362 and Q408 might also play a role in AlgX binding to alginate but that remains to be determined.

Chapter 5 - Conclusion

This dissertation investigated two distinct mechanisms that bacteria use to form persistent infections in humans, antibiotic resistance and biofilm production. Both mechanisms arise due to spontaneous mutations in the bacterial genome. Mutations in the genome occur because of selective pressures in the bacteria's micro-environment.

Amoxicillin resistance in Helicobacter pylori

In the case of *Helicobacter pylori*, mutations occur when *H. pylori* is exposed to amoxicillin; these mutations occur in various genes that enhance the bacterium's resistance to amoxicillin. This study identified 11 mutations in 9 genes that distinguish IS5, an in vitro evolved amoxicillin resistance strain, from 26695, a parental wild-type strain. Based on evaluation of available literature, this study narrowed its focus to the 7 mutations occurring in PBP1, PBP2, HopC, HefC, and HofH. Further investigation of these 7 mutations suggests that mutations in penicillin binding protein 1 (PBP1), outer membrane protein 20 (HopC), acriflavine resistance protein (HefC) and outer membrane protein 3 (HofH) were responsible for a majority of the resistance observed in the IS5 strain. With the exception of HopC, each of these mutated genes was individually transformed into the sensitive 26695 strain and resulted in a significant increase in amoxicillin resistance.

PBP1 contained two mutations believed to enhance amoxicillin resistance. During the first stage of resistance, IS1, PBP1 is mutated at P372S. The impact of this mutation is not as obvious as other published mutations that occur within the binding pocket and physically protrude into the amoxicillin binding cleft[101]. However, among

the other mutations occurring in the IS1 strain (Table 1), this PBP1 mutation is the most likely to contribute to the increased amoxicillin resistance. This mutation occurs near the previously identified β-lactam binding pocket[101, 109, 143] and conceivably alters the structure of the binding pocket, reducing amoxicillin binding. During the fourth stage of resistance, IS4, the second mutation in PBP1 occurs. This T438M mutation was previously reported to significantly contribute to amoxicillin resistance[96]. It is speculated that the mutation causes a protrusion into the binding pocket and restricts amoxicillin binding. This mutation was the only new mutation to occur in IS4, further supporting its contribution to amoxicillin resistance.

The HopC mutation, R302H, could not be transformed into the sensitive 26695 strain. Previously, other mutations in Hop proteins, including HopC, have been associated with amoxicillin resistance[96]. The previously observed HopC mutation, a 211 nonsense mutation, was associated with a 0.125 mg/L amoxicillin MIC, a marginal 2-fold increase over the parental sensitive strain. When the HopC nonsense mutation was combined with a PBP1 mutation, the two synergize for a 1.0 mg/L amoxicillin MIC, a significant 8-fold increase. While the HopC R302H SNP alone was not isolated, it is possible that the HopC SNP synergizes with the IS1 PBP1 mutation and significantly increases amoxicillin resistance.

Very little is known about the putative outer membrane protein 2, HofH. This study is the first to suggest that a G228W mutation in HofH has an impact on amoxicillin sensitivity. The G228W HofH mutation causes a 16-fold increase over the 26695 parental amoxicillin MIC. HofH joins other outer membrane proteins, including HopC and

HopB in *Helicobacter pylori*[96], which are sensitive to spontaneous mutations that result in reduced antibiotic uptake. Mutations in outer membrane proteins, such as HofH, have a profound impact on hydrophilic antibiotics, like β-lactams, that depend primarily on outer membrane transmembrane protein channels for cellular uptake.

The HefC L378F mutation occurring in IS3 is speculated to impact the amoxicillin resistance of IS3, IS4 and IS5. HefC is believed to resemble the MexB component of a multidrug resistance (MDR) efflux pump consisting of MexA-B and OprM. Efflux of various antibiotics has been associated with resistance in a variety of bacteria. Efflux in *Helicobacter pylori* has been linked with metronidazole, penicillin, and clarithromycin resistance, but not amoxicillin[98, 99, 116, 144]. Remarkably, this study has demonstrated that the observed HefC mutation enhances the pumps function, an unexpected but not unprecedented effect[145].

Ultimately, this dissertation has demonstrated that 4 of the 5 mutations mentioned above directly impact amoxicillin resistance and has provided evidence to support the role of the fifth mutation (HopC). These 5 mutations are believed to account for a majority of the resistance observed in the in vitro selected IS5 strain used for this study.

Biofilm production in Pseudomonas aeruginosa

The biosynthesis of alginate, a secreted exopolysaccharide biofilm, forms a protective barrier that allows *Pseudomonas aeruginosa* to form a chronic infection in CF patients. It is thought that a portion of the proteins produced by the alginate biosynthetic operon form a multi-protein biosynthetic complex within the periplasm (Figure 2). This

dissertation aimed to identify the contribution of AlgL and AlgX to the multi-protein biosynthetic complex and alginate biosynthesis.

The role of AlgL during alginate biosynthesis

Investigation of AlgL, a periplasmic endomannuronic alginate lyase, began with the creation of an AlgL knockout in a clinically derived strain, FRD1050. The FRD1050 strain contains all the essential alginate biosynthetic machinery under the control of an IPTG inducible promoter. This study's attempt to create an *algL* knockout produced two strains with distinct phenotypes when induced - a viable, non-alginate producing strain and a lethal, alginate producing strain. In-trans complementation by *algL* recovered the viability and alginate production of the IPTG inducible lethal knockout but not the IPTG inducible viable knockout. Attempts to express two different catalytically inactive AlgL proteins in the IPTG inducible lethal knockout were not able to recover viability. This suggested that lyase activity was essential to cell survival. Surprisingly, alginate production in the IPTG inducible lethal knockout was recovered by catalytically inactive AlgL complementations. This indicated that AlgL activity was not required for alginate production and that AlgL might aid alginate biosynthesis as part of the multi-protein biosynthetic complex.

Attempts to identify protein-protein interactions were done using co-immunoprecipitation of DSS crosslinked protein samples. Samples were isolated from an IPTG inducible lethal knockout culture recovered by expression of AlgL-HA in-trans. Crosslinked samples were analyzed by western blot and MudPIT MS-MS. Unfortunately,

none of the proposed components of the multi-protein biosynthetic complex were identified. Though this suggests that AlgL does not interact with the multi-protein biosynthetic complex, the recovery of alginate production from the induced lethal knockout using catalytically inactive AlgL protein suggests otherwise. In short, this project remains unfinished. It is clear that AlgL is essential for cell survival and is not required for mannuronic acid polymerization. Further work needs to address the possible interaction of AlgL with the multi-protein biosynthetic complex and explain why catalytically inactive AlgL recovers alginate production.

The significance of AlgX carbohydrate binding module amino acids

Early AlgX studies demonstrated that it was essential for full-length alginate biosynthesis but the actual role for AlgX was elusive. A recent AlgX study has shown that AlgX plays a role in mannuronic acid acetylation[49], a role previously attributed only to AlgI-J-F. Analysis of the protein structure identified a C-terminal carbohydrate-binding module (CBM), which is presumably essential to alginate binding and biosynthesis. Based on the protein structure, this dissertation attempted to identify amino acids critical to alginate binding and assess their impact on alginate biosynthesis.

Docking studies with various uronic acid polymers were used to assess the theoretical involvement of CBM amino acids in binding to the polymers. Of the 6 amino acids theoretically involved in binding the polymer by the structural study[49], K396, R406 and K410 were predicted to interact with docked polymer. T398 and W400 were not predicted to interact with the docked polymers and R364 was unpredictable. Docked polymers containing both mannuronic acids and guluronic acids were predicted to form

significantly more interactions than polymers consisting of all mannuronic acids. This suggests that epimerization by AlgG might precede acetylation.

Alanine mutations of the 6 theoretical amino acids identified by the structural study{Riley, 2013 #520} were created to examine the impact that each might have on alginate binding and alginate biosynthesis. Retention of enriched AlgX-His was measured on an alginate conjugated sepharose column. AlgX-His with mutations T398A and R406A were unable to bind to the alginate conjugated columns. AlgX-His with the W400A mutation demonstrated a significant increase in retention during column washes, 0.7±0.2% (W400A) compared to 16.7±3.6% (all others). R364A, K396A, K410A had no impact on AlgX retention by the alginate conjugated column.

Similarly, FRD1050 *algX* knockouts expressing AlgX-His with T398A and R406A mutations were unable to recover HMW uronic acid biosynthesis. These findings suggest that AlgX-His with either T398A or R406A mutations are unable to bind alginate and prevents alginate biosynthesis. Interestingly, expression of AlgX-His W400A in an *algX* knockout was also unable to recover HMW uronic acid biosynthesis. Considering higher retention of AlgX-His W400A in column washes, it seems likely that AlgX-His W400A is unable to release the bound polymer, thus blocking further alginate biosynthesis. Expression of R364A, K396A and K410A were able to recover the biosynthesis of HMW uronic acid polymers.

Ultimately, this study was able to identify 3 amino acids, T398, W400 and R406 that appear to be important to alginate binding and alginate biosynthesis. There might be

other amino acids, including Q362 and E444 that contribute to alginate binding and biosynthesis.

Refences

1. Donaldson, S. and R. Boucher, *Pathophysiology of cystic fibrosis.* Annales Nestlé (English ed.), 2007. **64**(3): p. 101-109.

2. Guggino, W.B. and S.P. Banks-Schlegel, *Macromolecular interactions and ion transport in cystic fibrosis.* Am J Respir Crit Care Med, 2004. **170**(7): p. 815-20.

3. Stutts, M.J., et al., *Cftr as a Camp-Dependent Regulator of Sodium-Channels.* Science, 1995. **269**(5225): p. 847-850.

4. Cheng, S.H., et al., *Phosphorylation of the R domain by cAMP-dependent protein kinase regulates the CFTR chloride channel.* Cell, 1991. **66**(5): p. 1027-36.

5. Travis, S.M., H.A. Berger, and M.J. Welsh, *Protein phosphatase 2C dephosphorylates and inactivates cystic fibrosis transmembrane conductance regulator.* Proc Natl Acad Sci U S A, 1997. **94**(20): p. 11055-60.

6. Ratjen, F. and G. Doring, *Cystic fibrosis.* Lancet, 2003. **361**(9358): p. 681-9.

7. *Correlation between genotype and phenotype in patients with cystic fibrosis. The Cystic Fibrosis Genotype-Phenotype Consortium.* N Engl J Med, 1993. **329**(18): p. 1308-13.

8. McKone, E.F., et al., *Effect of genotype on phenotype and mortality in cystic fibrosis: a retrospective cohort study.* Lancet, 2003. **361**(9370): p. 1671-6.

9. Mickle, J.E. and G.R. Cutting, *Genotype-phenotype relationships in cystic fibrosis.* Med Clin North Am, 2000. **84**(3): p. 597-607.

10. Katkin, J. *Cystic fibrosis: Genetics and pathogenesis*. [Online] 2014 Oct 2 2013 March 31 2014].

11. Gibson, R.L., J.L. Burns, and B.W. Ramsey, *Pathophysiology and management of pulmonary infections in cystic fibrosis.* Am J Respir Crit Care Med, 2003. **168**(8): p. 918-51.

12. Kanj, S. and D. Sexton. *Epidemiology, microbiology, and pathogenesis of Pseudomonas aeruginosa infection*. 2014 Oct 17, 2013 April 1st, 2014].

13. Li, Z., et al., *Longitudinal development of mucoid Pseudomonas aeruginosa infection and lung disease progression in children with cystic fibrosis.* JAMA, 2005. **293**(5): p. 581-8.

14. Fick, R.B., Jr., F. Sonoda, and D.B. Hornick, *Emergence and persistence of Pseudomonas aeruginosa in the cystic fibrosis airway.* Semin Respir Infect, 1992. **7**(3): p. 168-78.

15. Rodriguez-Rojas, A., A. Oliver, and J. Blazquez, *Intrinsic and environmental mutagenesis drive diversification and persistence of Pseudomonas aeruginosa in chronic lung infections.* J Infect Dis, 2012. **205**(1): p. 121-7.

16. Oliver, A., et al., *High frequency of hypermutable Pseudomonas aeruginosa in cystic fibrosis lung infection.* Science, 2000. **288**(5469): p. 1251-4.

17. Oliver, A. and A. Mena, *Bacterial hypermutation in cystic fibrosis, not only for antibiotic resistance.* Clin Microbiol Infect, 2010. **16**(7): p. 798-808.

18. Hogardt, M. and J. Heesemann, *Adaptation of Pseudomonas aeruginosa during persistence in the cystic fibrosis lung.* Int J Med Microbiol, 2010. **300**(8): p. 557-62.

19. Hogardt, M., et al., *Stage-specific adaptation of hypermutable Pseudomonas aeruginosa isolates during chronic pulmonary infection in patients with cystic fibrosis.* J Infect Dis, 2007. **195**(1): p. 70-80.

20. Smith, E.E., et al., *Genetic adaptation by Pseudomonas aeruginosa to the airways of cystic fibrosis patients.* Proc Natl Acad Sci U S A, 2006. **103**(22): p. 8487-92.

21. Qiu, D., et al., *ClpXP proteases positively regulate alginate overexpression and mucoid conversion in Pseudomonas aeruginosa.* Microbiology, 2008. **154**(Pt 7): p. 2119-30.

22. Lamppa, J.W., et al., *Genetically engineered alginate lyase-PEG conjugates exhibit enhanced catalytic function and reduced immunoreactivity.* PLoS One, 2011. **6**(2): p. e17042.

23. Rehm, B.H. and S. Valla, *Bacterial alginates: biosynthesis and applications.* Appl Microbiol Biotechnol, 1997. **48**(3): p. 281-8.

24. Paletta, J.L. and D.E. Ohman, *Evidence for two promoters internal to the alginate biosynthesis operon in Pseudomonas aeruginosa.* Curr Microbiol, 2012. **65**(6): p. 770-5.

25. Hay, I.D., et al., *Bacterial biosynthesis of alginates.* Journal of chemical technology and biotechnology, 2010. **85**(6): p. 752-759.

26. Hay, I.D., et al., *Genetics and regulation of bacterial alginate production.* Environ Microbiol, 2014.

27. Zielinski, N.A., A.M. Chakrabarty, and A. Berry, *Characterization and regulation of the Pseudomonas aeruginosa algC gene encoding phosphomannomutase.* J Biol Chem, 1991. **266**(15): p. 9754-63.

28. Deretic, V., J.F. Gill, and A.M. Chakrabarty, *Gene algD coding for GDPmannose dehydrogenase is transcriptionally activated in mucoid Pseudomonas aeruginosa.* J Bacteriol, 1987. **169**(1): p. 351-8.

29. Maharaj, R., et al., *Sequence of the alg8 and alg44 genes involved in the synthesis of alginate by Pseudomonas aeruginosa.* Gene, 1993. **136**(1-2): p. 267-9.

30. Rehman, Z.U., et al., *Insights into the assembly of the alginate biosynthesis machinery in Pseudomonas aeruginosa.* Appl Environ Microbiol, 2013. **79**(10): p. 3264-72.

31. Chitnis, C.E. and D.E. Ohman, *Cloning of Pseudomonas aeruginosa algG, which controls alginate structure.* J Bacteriol, 1990. **172**(6): p. 2894-900.

32. Franklin, M.J., et al., *Pseudomonas aeruginosa AlgG is a polymer level alginate C5-mannuronan epimerase.* J Bacteriol, 1994. **176**(7): p. 1821-30.

33. Franklin, M.J. and D.E. Ohman, *Mutant analysis and cellular localization of the AlgI, AlgJ, and AlgF proteins required for O acetylation of alginate in Pseudomonas aeruginosa.* J Bacteriol, 2002. **184**(11): p. 3000-7.

34. Franklin, M.J. and D.E. Ohman, *Identification of algF in the alginate biosynthetic gene cluster of Pseudomonas aeruginosa which is required for alginate acetylation.* J Bacteriol, 1993. **175**(16): p. 5057-65.

35. Keiski, C.L., et al., *AlgK is a TPR-containing protein and the periplasmic component of a novel exopolysaccharide secretin.* Structure, 2010. **18**(2): p. 265-73.

36. Monday, S.R. and N.L. Schiller, *Alginate synthesis in Pseudomonas aeruginosa: the role of AlgL (alginate lyase) and AlgX.* J Bacteriol, 1996. **178**(3): p. 625-32.

37. Jain, S. and D.E. Ohman, *Role of an alginate lyase for alginate transport in mucoid Pseudomonas aeruginosa.* Infect Immun, 2005. **73**(10): p. 6429-36.

38. Albrecht, M.T. and N.L. Schiller, *Alginate lyase (AlgL) activity is required for alginate biosynthesis in Pseudomonas aeruginosa.* J Bacteriol, 2005. **187**(11): p. 3869-72.

39. Robles-Price, A., et al., *AlgX is a periplasmic protein required for alginate biosynthesis in Pseudomonas aeruginosa.* J Bacteriol, 2004. **186**(21): p. 7369-77.

40. Jain, S. and D.E. Ohman, *Deletion of algK in mucoid Pseudomonas aeruginosa blocks alginate polymer formation and results in uronic acid secretion.* J Bacteriol, 1998. **180**(3): p. 634-41.

41. Seiderer, L., R. Newell, and P. Cook, *Quantitative significance of style enzymes from two marine mussels (Choromytilus meridionalis Krauss and Perna perna Linnaeus) in relation to diet.* Marine biology letters, 1982.

42. Russell, N.J. and P. Gacesa, *Chemistry and biology of the alginate of mucoid strains of Pseudomonas aeruginosa in cystic fibrosis.* Mol Aspects Med, 1988. **10**(1): p. 1-91.

43. Kim, H.S., C.-G. Lee, and E.Y. Lee, *Alginate lyase: Structure, property, and application.* Biotechnology and Bioprocess Engineering, 2011. **16**(5): p. 843-851.

44. Yoon, H.J., et al., *Crystal structure of alginate lyase A1-III complexed with trisaccharide product at 2.0 A resolution.* J Mol Biol, 2001. **307**(1): p. 9-16.

45. Yoon, H.J., et al., *Crystal structure of alginate lyase A1-III from Sphingomonas species A1 at 1.78 A resolution.* J Mol Biol, 1999. **290**(2): p. 505-14.

46. Zhang, Z., et al., *Preparation and structure elucidation of alginate oligosaccharides degraded by alginate lyase from Vibro sp. 510.* Carbohydr Res, 2004. **339**(8): p. 1475-81.

47. Schiller, N.L., et al., *Characterization of the Pseudomonas aeruginosa alginate lyase gene (algL): cloning, sequencing, and expression in Escherichia coli.* J Bacteriol, 1993. **175**(15): p. 4780-9.

48. May, T.B. and A.M. Chakrabarty, *Pseudomonas aeruginosa: genes and enzymes of alginate synthesis.* Trends Microbiol, 1994. **2**(5): p. 151-7.

49. Riley, L.M., et al., *Structural and functional characterization of Pseudomonas aeruginosa AlgX: role of AlgX in alginate acetylation.* J Biol Chem, 2013. **288**(31): p. 22299-314.

50. Linz, B., et al., *An African origin for the intimate association between humans and Helicobacter pylori.* Nature, 2007. **445**(7130): p. 915-8.

51. Falush, D., et al., *Traces of human migrations in Helicobacter pylori populations.* Science, 2003. **299**(5612): p. 1582-5.

52. Ghose, C., et al., *East Asian genotypes of Helicobacter pylori strains in Amerindians provide evidence for its ancient human carriage.* Proc Natl Acad Sci U S A, 2002. **99**(23): p. 15107-11.

53. Marshall, B.J. and J.R. Warren, *Unidentified curved bacilli on gastric epithelium in active chronic gastritis.* Lancet, 1983. **1**(8336): p. 1273-5.

54. Marshall, B.J. and J.R. Warren, *Unidentified curved bacilli in the stomach of patients with gastritis and peptic ulceration.* Lancet, 1984. **1**(8390): p. 1311-5.

55. Marshall, B.J., et al., *Attempt to fulfil Koch's postulates for pyloric Campylobacter.* Med J Aust, 1985. **142**(8): p. 436-439.

56. Brown, L.M., *Helicobacter pylori: epidemiology and routes of transmission.* Epidemiol Rev, 2000. **22**(2): p. 283-97.

57. Pounder, R.E. and D. Ng, *The prevalence of Helicobacter pylori infection in different countries.* Aliment Pharmacol Ther, 1995. **9 Suppl 2**: p. 33-9.

58. Goodwin, C.S. and B.W. Worsley, *Microbiology of Helicobacter pylori.* Gastroenterol Clin North Am, 1993. **22**(1): p. 5-19.

59. Everhart, J.E., et al., *Seroprevalence and ethnic differences in Helicobacter pylori infection among adults in the United States.* J Infect Dis, 2000. **181**(4): p. 1359-63.

60. Smoak, B.L., P.W. Kelley, and D.N. Taylor, *Seroprevalence of Helicobacter pylori infections in a cohort of US Army recruits.* Am J Epidemiol, 1994. **139**(5): p. 513-9.

61. Torres, J., et al., *A community-based seroepidemiologic study of Helicobacter pylori infection in Mexico.* J Infect Dis, 1998. **178**(4): p. 1089-94.

62. Parsonnet, J., *The incidence of Helicobacter pylori infection.* Aliment Pharmacol Ther, 1995. **9 Suppl 2**: p. 45-51.

63. Kivi, M., et al., *Helicobacter pylori status in family members as risk factors for infection in children.* Epidemiology and infection, 2005. **133**(04): p. 645-652.

64. Webb, P., et al., *Relation between infection with Helicobacter pylori and living conditions in childhood: evidence for person to person transmission in early life.* Bmj, 1994. **308**(6931): p. 750-753.

65. Hunt, R.H., K. Sumanac, and J.Q. Huang, *Review article: should we kill or should we save Helicobacter pylori?* Aliment Pharmacol Ther, 2001. **15 Suppl 1**: p. 51-9.

66. Suerbaum, S. and P. Michetti, *Medical progress: Helicobacter pylori infection.* New England Journal of Medicine, 2002. **347**(15): p. 1175-1186.

67. Weeks, D.L., et al., *A H+-gated urea channel: the link between Helicobacter pylori urease and gastric colonization.* Science, 2000. **287**(5452): p. 482-5.

68. Mobley, H.L., *The role of Helicobacter pylori urease in the pathogenesis of gastritis and peptic ulceration.* Aliment Pharmacol Ther, 1996. **10 Suppl 1**: p. 57-64.

69. Ilver, D., et al., *Helicobacter pylori adhesin binding fucosylated histo-blood group antigens revealed by retagging.* Science, 1998. **279**(5349): p. 373-377.

70. Mobley, H.L., *Defining Helicobacter pylori as a pathogen: strain heterogeneity and virulence.* Am J Med, 1996. **100**(5A): p. 2S-9S; discussion 9S-11S.

71. Logan, R.P., *Adherence of Helicobacter pylori.* Aliment Pharmacol Ther, 1996. **10 Suppl 1**: p. 3-15.

72. Szabo, I., et al., *Formation of anion-selective channels in the cell plasma membrane by the toxin VacA of Helicobacter pylori is required for its biological activity.* Embo Journal, 1999. **18**(20): p. 5517-5527.

73. Galmiche, A., et al., *The N-terminal 34 kDa fragment of Helicobacter pylori vacuolating cytotoxin targets mitochondria and induces cytochrome c release.* Embo Journal, 2000. **19**(23): p. 6361-6370.

74. Fan, X., et al., *Helicobacter pylori urease binds to class II MHC on gastric epithelial cells and induces their apoptosis.* J Immunol, 2000. **165**(4): p. 1918-24.

75. Goodwin, C.S., J.A. Armstrong, and B.J. Marshall, *Campylobacter pyloridis, gastritis, and peptic ulceration.* J Clin Pathol, 1986. **39**(4): p. 353-65.

76. Chey, W.D., B.C. Wong, and G. Practice Parameters Committee of the American College of, *American College of Gastroenterology guideline on the management of Helicobacter pylori infection.* Am J Gastroenterol, 2007. **102**(8): p. 1808-25.

77. McColl, K.E., *Clinical practice. Helicobacter pylori infection.* N Engl J Med, 2010. **362**(17): p. 1597-604.

78. Dunn, B.E., H. Cohen, and M.J. Blaser, *Helicobacter pylori.* Clin Microbiol Rev, 1997. **10**(4): p. 720-41.

79. Francavilla, R., et al., *Clarithromycin-resistant genotypes and eradication of Helicobacter pylori.* J Pediatr, 2010. **157**(2): p. 228-32.

80. Bjorkholm, B., et al., *Mutation frequency and biological cost of antibiotic resistance in Helicobacter pylori.* Proc Natl Acad Sci U S A, 2001. **98**(25): p. 14607-12.

81. Wang, G., M.Z. Humayun, and D.E. Taylor, *Mutation as an origin of genetic variability in Helicobacter pylori.* Trends Microbiol, 1999. **7**(12): p. 488-93.

82. Tsuda, M., M. Karita, and T. Nakazawa, *Genetic transformation in Helicobacter pylori.* Microbiol Immunol, 1993. **37**(1): p. 85-9.

83. Edwards, D.I., *Nitroimidazole drugs--action and resistance mechanisms. I. Mechanisms of action.* J Antimicrob Chemother, 1993. **31**(1): p. 9-20.

84. Muller, M., *Reductive activation of nitroimidazoles in anaerobic microorganisms.* Biochem Pharmacol, 1986. **35**(1): p. 37-41.

85. Tocher, J.H. and D.I. Edwards, *The interaction of reduced metronidazole with DNA bases and nucleosides.* Int J Radiat Oncol Biol Phys, 1992. **22**(4): p. 661-3.

86. Tocher, J.H. and D.I. Edwards, *Evidence for the direct interaction of reduced metronidazole derivatives with DNA bases.* Biochem Pharmacol, 1994. **48**(6): p. 1089-94.

87. Jeong, J.Y., et al., *Roles of FrxA and RdxA nitroreductases of Helicobacter pylori in susceptibility and resistance to metronidazole.* J Bacteriol, 2001. **183**(17): p. 5155-62.

88. Walsh, C., *Antibiotics: actions, origins, resistance*. 2003: American Society for Microbiology (ASM).

89. Megraud, F., *Epidemiology and mechanism of antibiotic resistance in Helicobacter pylori.* Gastroenterology, 1998. **115**(5): p. 1278-82.

90. Schnappinger, D. and W. Hillen, *Tetracyclines: antibiotic action, uptake, and resistance mechanisms.* Arch Microbiol, 1996. **165**(6): p. 359-69.

91. Li, X.Z., D.M. Livermore, and H. Nikaido, *Role of efflux pump(s) in intrinsic resistance of Pseudomonas aeruginosa: resistance to tetracycline, chloramphenicol, and norfloxacin.* Antimicrob Agents Chemother, 1994. **38**(8): p. 1732-41.

92. Li, X.Z., H. Nikaido, and K. Poole, *Role of mexA-mexB-oprM in antibiotic efflux in Pseudomonas aeruginosa.* Antimicrob Agents Chemother, 1995. **39**(9): p. 1948-53.

93. Pitout, J.D., C.C. Sanders, and W.E. Sanders, Jr., *Antimicrobial resistance with focus on beta-lactam resistance in gram-negative bacilli.* Am J Med, 1997. **103**(1): p. 51-9.

94. Calderwood, S.B. *Beta-lactam antibiotics: Mechanisms of action and resistance and adverse effects*. July 29, 2013 March 31 2014]; Available from: Final version of Brandon's thesis 7.17.14.docx.

95. DeLoney, C.R. and N.L. Schiller, *Competition of various beta-lactam antibiotics for the major penicillin-binding proteins of Helicobacter pylori: antibacterial activity and effects on bacterial morphology.* Antimicrob Agents Chemother, 1999. **43**(11): p. 2702-9.

96. Co, E.M. and N.L. Schiller, *Resistance mechanisms in an in vitro-selected amoxicillin-resistant strain of Helicobacter pylori.* Antimicrob Agents Chemother, 2006. **50**(12): p. 4174-6.

97. Bina, J.E., et al., *Helicobacter pylori uptake and efflux: basis for intrinsic susceptibility to antibiotics in vitro.* Antimicrob Agents Chemother, 2000. **44**(2): p. 248-54.

98. Hirata, K., et al., *Contribution of efflux pumps to clarithromycin resistance in Helicobacter pylori.* J Gastroenterol Hepatol, 2010. **25 Suppl 1**: p. S75-9.

99. Kutschke, A. and B.L. de Jonge, *Compound efflux in Helicobacter pylori.* Antimicrob Agents Chemother, 2005. **49**(7): p. 3009-10.

100. DeLoney, C.R. and N.L. Schiller, *Characterization of an In vitro-selected amoxicillin-resistant strain of Helicobacter pylori.* Antimicrob Agents Chemother, 2000. **44**(12): p. 3368-73.

101. Qureshi, N.N., D. Morikis, and N.L. Schiller, *Contribution of specific amino acid changes in penicillin binding protein 1 to amoxicillin resistance in clinical Helicobacter pylori isolates.* Antimicrob Agents Chemother, 2011. **55**(1): p. 101-9.

102. Rimbara, E., et al., *Correlation between substitutions in penicillin-binding protein 1 and amoxicillin resistance in Helicobacter pylori.* Microbiol Immunol, 2007. **51**(10): p. 939-44.

103. Rimbara, E., et al., *Mutations in penicillin-binding proteins 1, 2 and 3 are responsible for amoxicillin resistance in Helicobacter pylori.* J Antimicrob Chemother, 2008. **61**(5): p. 995-8.

104. Kurata, J.H. and B.M. Haile, *Epidemiology of peptic ulcer disease.* Clin Gastroenterol, 1984. **13**(2): p. 289-307.

105. Nishizawa, T., et al., *Enhancement of amoxicillin resistance after unsuccessful Helicobacter pylori eradication.* Antimicrob Agents Chemother, 2011. **55**(6): p. 3012-4.

106. Kern, W.V., et al., *Effect of 1-(1-naphthylmethyl)-piperazine, a novel putative efflux pump inhibitor, on antimicrobial drug susceptibility in clinical isolates of Escherichia coli.* J Antimicrob Chemother, 2006. **57**(2): p. 339-43.

107. Tomb, J.F., et al., *The complete genome sequence of the gastric pathogen Helicobacter pylori.* Nature, 1997. **388**(6642): p. 539-47.

108. Wang, Y., K.P. Roos, and D.E. Taylor, *Transformation of Helicobacter pylori by chromosomal metronidazole resistance and by a plasmid with a selectable chloramphenicol resistance marker.* J Gen Microbiol, 1993. **139**(10): p. 2485-93.

109. Gerrits, M.M., et al., *Multiple mutations in or adjacent to the conserved penicillin-binding protein motifs of the penicillin-binding protein 1A confer amoxicillin resistance to Helicobacter pylori.* Helicobacter, 2006. **11**(3): p. 181-7.

110. Gerrits, M.M., et al., *Alterations in penicillin-binding protein 1A confer resistance to beta-lactam antibiotics in Helicobacter pylori.* Antimicrob Agents Chemother, 2002. **46**(7): p. 2229-33.

111. Kwon, D.H., et al., *High-level beta-lactam resistance associated with acquired multidrug resistance in Helicobacter pylori.* Antimicrob Agents Chemother, 2003. **47**(7): p. 2169-78.

112. Matteo, M.J., et al., *Helicobacter pylori amoxicillin heteroresistance due to point mutations in PBP-1A in isogenic isolates.* J Antimicrob Chemother, 2008. **61**(3): p. 474-7.

113. Okamoto, T., et al., *A change in PBP1 is involved in amoxicillin resistance of clinical isolates of Helicobacter pylori.* J Antimicrob Chemother, 2002. **50**(6): p. 849-56.

114. Paul, R., et al., *Mutations of the Helicobacter pylori genes rdxA and pbp1 cause resistance against metronidazole and amoxicillin.* Antimicrob Agents Chemother, 2001. **45**(3): p. 962-5.

115. Tseng, Y.S., et al., *Amoxicillin resistance with beta-lactamase production in Helicobacter pylori.* Eur J Clin Invest, 2009. **39**(9): p. 807-12.

116. Belzer, C., et al., *The Helicobacter hepaticus hefA gene is involved in resistance to amoxicillin.* Helicobacter, 2009. **14**(1): p. 72-9.

117. Sennhauser, G., et al., *Crystal structure of the multidrug exporter MexB from Pseudomonas aeruginosa.* J Mol Biol, 2009. **389**(1): p. 134-45.

118. Godoy, A.P., et al., *Differentially expressed genes in response to amoxicillin in Helicobacter pylori analyzed by RNA arbitrarily primed PCR.* FEMS Immunol Med Microbiol, 2007. **50**(2): p. 226-30.

119. Paulsen, I.T., M.H. Brown, and R.A. Skurray, *Proton-dependent multidrug efflux systems.* Microbiol Rev, 1996. **60**(4): p. 575-608.

120. Tornroth-Horsefield, S., et al., *Crystal structure of AcrB in complex with a single transmembrane subunit reveals another twist.* Structure, 2007. **15**(12): p. 1663-73.

121. Hamosh, A., et al., *Comparison of the clinical manifestations of cystic fibrosis in black and white patients.* J Pediatr, 1998. **132**(2): p. 255-9.

122. Goldberg, J.B. and D.E. Ohman, *Cloning and expression in Pseudomonas aeruginosa of a gene involved in the production of alginate.* J Bacteriol, 1984. **158**(3): p. 1115-21.

123. Schweizer, H.P. and T.T. Hoang, *An improved system for gene replacement and xylE fusion analysis in Pseudomonas aeruginosa.* Gene, 1995. **158**(1): p. 15-22.

124. Hoshino, T. and M. Kageyama, *Purification and properties of a binding protein for branched-chain amino acids in Pseudomonas aeruginosa.* J Bacteriol, 1980. **141**(3): p. 1055-63.

125. Hurwitz, J. and A. Weissbach, *The formation of 2-keto-3-deoxyheptonic acid in extracts of Escherichia coli B. II. Enzymic studies.* J Biol Chem, 1959. **234**(4): p. 710-2.

126. Knutson, C.A. and A. Jeanes, *A new modification of the carbazole analysis: application to heteropolysaccharides.* Anal Biochem, 1968. **24**(3): p. 470-81.

127. Dische, Z., *Carbazole method for uronic acid.* J. Biol. Chem, 1947. **167**: p. 189-195.

128. EMBL. *Preparation of electrocompent E. coli cells*. Transformation of competent E. coli cells; Available from: https://http://www.embl.de/pepcore/pepcore_services/cloning/transformation/index.html.

129. Gallagher, S.R., *One-dimensional SDS gel electrophoresis of proteins.* Curr Protoc Protein Sci, 2012. **Chapter 10**: p. Unit 10 1 1-44.

130. Preston, L.A., et al., *Characterization of alginate lyase from Pseudomonas syringae pv. syringae.* J Bacteriol, 2000. **182**(21): p. 6268-71.

131. Songqin, P., *IIGB Proteomics Workshop*, in *Songqin, P.*, U.o.C.a. Riverside, Editor. 2011, Songqin, P.: UCR.

132. Drakakaki, G., et al., *Isolation and proteomic analysis of the SYP61 compartment reveal its role in exocytic trafficking in Arabidopsis.* Cell Res, 2012. **22**(2): p. 413-24.

133. Bradford, M.M., *A rapid and sensitive method for the quantitation of microgram quantities of protein utilizing the principle of protein-dye binding.* Anal Biochem, 1976. **72**: p. 248-54.

134. Gutsche, J., U. Remminghorst, and B.H. Rehm, *Biochemical analysis of alginate biosynthesis protein AlgX from Pseudomonas aeruginosa: purification of an AlgX-MucD (AlgY) protein complex.* Biochimie, 2006. **88**(3-4): p. 245-51.

135. Foundation, C.F., *Cystic Fibrosis Foundation Patient Registry: annual data report 2011.* 2011.

136. Weadge, J.T., et al., *Expression, purification, crystallization and preliminary X-ray analysis of Pseudomonas aeruginosa AlgX.* Acta Crystallogr Sect F Struct Biol Cryst Commun, 2010. **66**(Pt 5): p. 588-91.

137. Trott, O. and A.J. Olson, *AutoDock Vina: improving the speed and accuracy of docking with a new scoring function, efficient optimization, and multithreading.* J Comput Chem, 2010. **31**(2): p. 455-61.

138. Rozeboom, H.J., et al., *Structural and mutational characterization of the catalytic A-module of the mannuronan C-5-epimerase AlgE4 from Azotobacter vinelandii.* J Biol Chem, 2008. **283**(35): p. 23819-28.

139. Momma, K., et al., *Direct evidence for Sphingomonas sp. A1 periplasmic proteins as macromolecule-binding proteins associated with the ABC transporter: molecular insights into alginate transport in the periplasm.* Biochemistry, 2005. **44**(13): p. 5053-64.

140. Morris, G.M., et al., *AutoDock4 and AutoDockTools4: Automated docking with selective receptor flexibility.* J Comput Chem, 2009. **30**(16): p. 2785-91.

141. Diver, J.M., L.E. Bryan, and P.A. Sokol, *Transformation of Pseudomonas aeruginosa by electroporation.* Anal Biochem, 1990. **189**(1): p. 75-9.

142. Pedersen, S.S., et al., *Purification, characterization, and immunological cross-reactivity of alginates produced by mucoid Pseudomonas aeruginosa from patients with cystic fibrosis.* J Clin Microbiol, 1989. **27**(4): p. 691-9.

143. Contreras-Martel, C., et al., *Crystal structure of penicillin-binding protein 1a (PBP1a) reveals a mutational hotspot implicated in beta-lactam resistance in Streptococcus pneumoniae.* J Mol Biol, 2006. **355**(4): p. 684-96.

144. van Amsterdam, K., A. Bart, and A. van der Ende, *A Helicobacter pylori TolC efflux pump confers resistance to metronidazole.* Antimicrob Agents Chemother, 2005. **49**(4): p. 1477-82.

145. Bohnert, J.A., et al., *Altered spectrum of multidrug resistance associated with a single point mutation in the Escherichia coli RND-type MDR efflux pump YhiV (MdtF).* J Antimicrob Chemother, 2007. **59**(6): p. 1216-22.